BENTHAM SCIENCE

CrossMark

Current Medical Imaging

Content list available at: https://benthamscience.com/journals/cmir

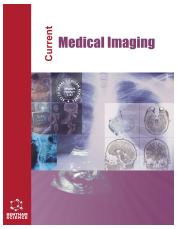

REVIEW ARTICLE

A Comprehensive Review on MRI-based Knee Joint Segmentation and Analysis Techniques

Pavan Mahendrakar[1,*], Dileep kumar[2] and Uttam Patil[3]

[1]*BLDEA's V.P.Dr. P.G., Halakatti College of Engineering and Technology, Vijayapur, Karnataka, India*
[2]*United Imaging Healthcare, Shanghai, China*
[3]*Jain College of Engineering, T.S Nagar, Hunchanhatti Road, Machhe, Belagavi, Karnataka, India*

Abstract:

Using magnetic resonance imaging (MRI) in osteoarthritis pathogenesis research has proven extremely beneficial. However, it is always challenging for both clinicians and researchers to detect morphological changes in knee joints from magnetic resonance (MR) imaging since the surrounding tissues produce identical signals in MR studies, making it difficult to distinguish between them. Segmenting the knee bone, articular cartilage and menisci from the MR images allows one to examine the complete volume of the bone, articular cartilage, and menisci. It can also be used to assess certain characteristics quantitatively. However, segmentation is a laborious and time-consuming operation that requires sufficient training to complete correctly. With the advancement of MRI technology and computational methods, researchers have developed several algorithms to automate the task of individual knee bone, articular cartilage and meniscus segmentation during the last two decades. This systematic review aims to present available fully and semi-automatic segmentation methods for knee bone, cartilage, and meniscus published in different scientific articles. This review provides a vivid description of the scientific advancements to clinicians and researchers in this field of image analysis and segmentation, which helps the development of novel automated methods for clinical applications. The review also contains the recently developed fully automated deep learning-based methods for segmentation, which not only provides better results compared to the conventional techniques but also open a new field of research in Medical Imaging.

Keywords: Osteoarthritis (OA), Cartilage, Bone, Meniscus, Magnetic Resonance Image (MRI), Knee Joint, Automated segmentation.

Article History	Received: August 26, 2022	Revised: November 29, 2022	Accepted: December 28, 2022

1. INTRODUCTION

The knee is the largest joint in the human body, and because of this, it is the joint that allows for the most fluid transitions from one position to another. There is currently no known treatment that may effectively reverse the crippling effects of osteoarthritis (OA), a degenerative joint disease that affects more than 71 million individuals all over the globe.

In older people, osteoarthritis, sometimes known as OA, is a prevalent and debilitating disorder. The most common technological tool employed to monitor and evaluate the progression of an OA is magnetic resonance imaging (MRI). Despite the fact that MRI provides an effective analysis of knee joint anatomy, it is an expensive modality and routine clinical examinations are limited due to its non-availability.

Injuries to the meniscus, anomalies in the bone beneath the joint boundaries, and a lack of articular cartilage integrity may all contribute to the development of osteoarthritis (OA) of the knee [1]. Pre-structural and structural changes in tissues such as articular cartilage, synovial, fluid meniscus, and subchondral bones may be measured to detect early-stage osteoarthritis [2]. In the assessment of osteoarthritis, pre-structural/biochemical compositions (water content, proteoglycan content and collagen) are mainly measured in the articular cartilage (AC) tissue to diagnose the disease at early stages, followed by the measurement of anatomical (thickness, volume, surface area) changes that occurs either at early or during the progression stages.

Similarly, quantitative MR of the meniscus has been used to measure biochemical (collagen-PG) changes during the early onset of osteoarthritis followed by its morphological (flap or complex tears; meniscal maceration; or destruction) changes to monitor progression. Alterations in the subchondral bone might be used as an imaging biomarker to diagnose knee osteoarthritis symptoms [3 - 5]. It has been shown that

* Address correspondence to this author at the BLDEA's V.P.Dr. P.G., Halakatti College of Engineering and Technology, Vijayapur, Karnataka, India;
E-mail: pavandmahendrakar@gmail.com

magnetic resonance imaging, often known as MR imaging, is an effective tool for evaluating osteophytes, surface area abnormalities, and lesions most commonly seen in bone marrow as a method for monitoring the progression of OA [3].

Quantitative MRI can diagnose, assess, and monitor diseases such as osteoarthritis by identifying morphologic changes in the knee and calculating quantitative values such as T1 rho and T1/T2 relaxation times. However, the clinical application of quantitative MRI has been hindered by the requirement for time-consuming post-processing of images, particularly for segmenting the joint and musculoskeletal tissue [5]. The anterior compartment (AC) is segmented in most quantitative MR techniques, and a technique-specific map is formed. This map is then utilized to evaluate particular data from knee tissue [6, 7].

In many cases, the AC subdivision (whether for the entire system or individual compartments) is performed manually by a trained professional or semi-automatically. Both of these methods are laborious and time-consuming and potentially introduce dependability issues Neogi *et al*. [8]. If done manually, it can take a skilled technician around three hours to do an image, depending on the image's quality and what is being segmented. In order for doctors and scientists to develop biomarkers, knee implants, knee kinematics, and a comprehension of the physical phenomena that occur within healthy knee joints, segmenting the tissue that makes up the knee joint, such as the cartilage, the bones, and the meniscus, using medical images is an essential first step.

Segmentation of knee bone, articular cartilage and meniscus from MRI images knee segmentation is currently a popular area of research because it can save a significant amount of time being spent by doctors and radiologists in order to accurately a significant amount of time and effort while also improving the accuracy of their diagnose pathologies related to joint diseases. As a result, this area of study holds a great deal of promise for both clinical and scientific investigation. Thus, this comprehensive review focuses on the MRI-based knee joint segmentation methods and their impact on future technology development.

2. EXISTING METHODS

2.1. Bone Segmentation & Quantification of Changes

Segmentation of subchondral bone from MR images has two important aspects in knee OA studies; (1) to quantify alterations in the tibial plateau, bony surface contour (*e.g.*, subchondral bone attrition), bone shape, surface geometry and area from 3D model reconstructed from segmented bone regions as an imaging biomarker to monitor the progression of knee OA [8] and (2) as an intermediate stage in the segmentation of knee joint associated tissues like articular cartilage, meniscus, ligaments, *etc*. as bone being the larger size tissue in MR images, regular shape and more discriminative intensity as compared to other joint tissues [9, 10]. Various researchers have proposed techniques to segment the subchondral bones to fulfill the above-mentioned importance. Segmentation of the subchondral bones from MR images is a challenging task. Various researchers have proposed and investigated several promising knee bone segmentation algorithms, as summarized in Table **1**, with the type of MR sequence used.

Table 1. Automatic segmentation of bone: Existing studies (After the year 2010).

Type	Key Segmentation Algorithms	Author, Year & MRI Sequence	Performance Parameters	Dependability
-	Graph Cut Algorithm	Ababneh *et al*. 2011 [10] Sagittal T2 map	DSC – 0.95	-
Fully-automatic	Multi-atlas registration and voxel classification	Tamez-Pena *et al*. 2016 [11] Sequence not Specified	DSC (Femur) – 0.95 DSC (Tibia) – 0.95	Most algorithms depend on Models and Atlas designs, Training dataset set for classification
		Dam *et al*. 2015 [12] Sagittal Turbo MR sequence	DSC (Tibia) – 0.97	
	Ray Casting technique	Dodin *et al*. 2011 [13] Gradient echo fat suppressed sequence	DSC (Femur) – 0.94 DSC (Tibia) – 0.92	
	Random and Semantic Context Forests Learning	Balsiger *et al*. 2015 [14] Sequence not Specified	DSC (Femur) – 0.92	
		Wang *et al*. 2013 [15] DESS MR sequence	DSC (Femur) – 0.94 DSC (Tibia) – 0.95 DSC (Patella) – 0.94	
	Active and Statistical Shape Models, Appearance Models	Neogi *et al*. 2013 [8] DESS MR sequence	Not specified	
		Bindernagel *et al*. 2011 [16] Sequence not Specified	DSC (Femur) – 0.94 DSC (Tibia) – 0.89	
		Seim *et al*. 2010 [17] Sequence not Specified	AvgD (Femur) – 1.02 mm RMSD (Femur) – 1.54mm AvgD (Tibia) – 0.84 mm RMSD (Tibia) – 1.24 mm	
-	Continuous convex optimization	Shan *et al*. 2010 [18] T1 and T2* images	Not specified	Incorporating regional and shape information
Semi-automatic	Quantitative BML measurement	Ratzlaff *et al*. 2013 [19] 3 T TSE FS intermediate-weighted (IW) sequence	Tibia BML volume *vs*. WORMS scores	Weight-bearing pain was associated with BML volume

(Table 1) contd.....

Type	Key Segmentation Algorithms	Author, Year & MRI Sequence	Performance Parameters	Dependability
Fully automatic	2D and 3D CNN segmentation models	Deniz *et al*. 2018 [20] T1-weighted 3D fast low angle shot (3D FLASH) images	DSC-0.95	Multiple initial feature maps, layers and dilation rates
Fully automatic	Deformable model-based approach with automatic initial point selection to segment knee bones	Kim *et al*. 2018 [21], MRI datasets of kne from http://mridataweb.us-west-2.elasticbeanstalk.com	Results showed that the approach achieves 95% of Dice, 93% of SENS, and 99% of SPEC in the volume evaluation, whereas ASSD of 1.17mm and RMSD of 2.01mm in the surface evaluation.	3D deformable model
Fully automatic	CNN, 3D fully connected conditional random field (CRF)	Zhou *et al*. 2019 [22] T1-weighted spoiled gradient recalled-echo (3D-SPGR) knee images	Dice coefficients femur (mean ± SD: 0.970 ± 0.010), tibia (0.962 ± 0.015), muscle (0.932 ± 0.024), and other non-specified tissues (0.913 ± 0.017)	3D simplex deformable modelling
Fully automatic	Evaluate the cross-sectional and longitudinal association of BMLs	Roemer *et al*. 2010 [23] 1.0 T dedicated MR system with a circumferential extremity coil using fat-suppressed (fs) fast spin-echo proton density	1025 knees were included. 8.9% of the analyzed knee subregions showed SBA present at baseline, and 9.2% of subregions exhibited prevalent subchondral BMLs	With SBA in the same subregion of the knee
Fully automatic	Deep Siamese Convolutional Neural Network	Tiulpin *et al*. 2017 [24], two public datasets: MOST and OAI	-	The Kellgren-Lawrence grading scale
Fully automatic	Combining statistical shape knowledge and convolutional neural networks	Ambellan *et al*. 2019 [25], E, Siemens, Philips, Toshiba, Hitachi. Mostly 1.5T, some 3T, a few 1TSiemens 3T Trio Siemens 3T Trio MRI sequence: Many (T1, T2, GRE, Spoiled-GRE) partly with fat suppression, DESS, Acquisition plane: sagittal,	The DSC is 98.6% for FB, 98.5% for TB, 89.9% for FC, and 85.6% for TC.	SKI10 challenge, as well as from the OAI database
Fully automatic	Landmark-based shape regression and subsequent local segmentation of relevant areas.	Schock *et al*. 2020 [26], public dataset: OAI	Performance of existing high-precision approaches in terms of segmentation accuracy while at the same time drastically reducing computational complexity and improving runtime by a large margin.	OAI-ZIB dataset
Fully automatic	Douglas-Rachford splitting algorithm	Rini *et al*. 2020 [27], 1.5 T MR scanner with MR Images of size 512×512 pixels	The values of parameters such as DSC, specificity and sensitivity are 97.12%, 98.28% and 99.72% margin.	Douglas-Rachford Splitting algorithm.
Fully automatic	Multi-stage convolutional neural networks	Gatti 2020 [28] public dataset: OAI	The framework produces cartilage segmentation accuracies (Dice similarity coefficient) of 0.907 (femoral), 0.876 (medial tibial), 0.913 (lateral tibial), and 0.840 (patellar).	Multi-stage convolutional neural networks

(Table 1) contd.....

Type	Key Segmentation Algorithms	Author, Year & MRI Sequence	Performance Parameters	Dependability
Semi-automatic	Gradient-based semi-automatic bone segmentation algorithm	Heckelman, L.N. 2021 [29], 3.0 T MR scanner (TIM Trio; Siemens Healthcare; Malvern, PA) with an 8-channel knee coil (*In-vivo*; Gainesville, FL).	Dice similarity coefficient = 0.988 ± 0.002; surface distance = − 0.01 ± 0.001 mm	(1) repeated semi-automatic segmentations of the same T1 VIBE MRI scans, (2) semi-automatic segmentations of second T1 VIBE MRI scans of the same participants, and (3) manual segmentations of DESS MRI scans of the same participants.
Fully automated	Eagle algorithm	Rini *et al*. [30], 2021, three-dimensional (3-D) gradient-echo MR images of the knee	Improved accuracy in contrast with other traditional methods	Thickness of the cartilage region from the femur, tibia or patella bone and segment the portion.
Fully automated	2.5D U-N*et algorithm*	Robert *et al*. [31] 2022, SKI10 database from the MICCAI challenge	Final Dice score (98%) compared well with the state-of-the-art algorithms	SKI10 database from the MICCAI challenge and U Net 2.5 architecture.
Fully automated	A mask region-based convolutional neural network (RCNN) algorithm	Patekar *et al*. [32] 2022, public dataset:OAI	Improved dice similarity scores for femur bone 97.11%, tibia bone 97.33%, and patella bone 97.05% are obtained by Mask RCNN with Resnet-101 as backbone architecture.	Mask region-based convolutional neural network (RCNN) algorithm and Marching-Cube algorithm.

Abbreviations: DSC - Dice Similarity Coefficient, Sens.- Sensitivity, Spec. – Specificity, AvgD. – Average Surface distance, RMSD – Root mean square distance, Seg. Err. – Mean Segmentation Error

A three-dimensional MRI model of the knee's bone structure was demonstrated to assist in predicting the development of knee osteoarthritis in research conducted by Neogi *et al*. [8]. There will be research conducted to examine whether or not the 3D bone obtained from an MRI can accurately predict the onset of knee osteoarthritis (OA). The participants in this research consisted of two randomly picked patients and two randomly chosen controls. Both patient and control participants had acquired incident tibiofemoral radiographic knee osteoarthritis (OA). Through active appearance modelling of the femur, tibia, and patella, the author was able to find the best knees for OA classification using knee imaging throughout the study.

MRI texture analysis may detect changes in the subchondral bone in patients with OA. MacKay *et al*. [9] investigated whether or not there was a correlation between MRI texture analysis and histomorphometry in terms of osteoarthritic subchondral bone. The study includes 10 patients aged 57 to 84 scheduled to have total knee arthroplasty (TKA) undergone knee MR examination on 3T using high-resolution coronal T1 weighted sequencing. Tibial plateau explants were histologically created during TKA to assess bone volume fraction (BV.TV), trabecular thickness (Tb.Th), trabecular separation, and trabecular number. BV.TV stands for bone volume fraction, while Tb.Th stands for trabecular thickness (Tb.N). The authors used regression models to investigate the association between texture analysis features such as BV.TV, Tb.Th, Tb.Sp, and Tb.

Peña *et al*. [11] published the outcomes of an automated segmentation system for knee MRI images as well as the histological slices of the tibial subchondral bone. Authors were able to determine the degree to which the geographically overlapping areas of the automatically and manually separated segments by using the dice similarity coefficient (DSC). The DSC values obtained were 0.95 for both Tibia and Femur, showing good agreement between automated and manual segmentation.

An automated segmentation technique for MRIs of the knee was suggested by Dam *et al*. 2015 [12]. The framework uses a multi-atlas rigid registration and voxel classification as a consequence of training on a variety of segmentations of bones, cartilages, and menisci from a database of 1907 MRIs of the knee. When compared against manual reader re-segmentation, the performance of the re-segmentation was shown to be superior in terms of accuracy and precision.

An MR-based bone segmentation approach for the human knee has been developed by Dodin *et al*. [13] and focuses on femur and tibia segmentation in data from 161 patients. The authors used the ray casting method to locate the borders between bones in MR images acquired using gradient echo fat suppressed sequence. Results obtained in this study were compared with a validated semi-automatic segmentation technique. Results were compared in terms of the average surface distance (ASD), volume correlation coefficient (VC) and Dice similarity coefficient. Ray casting method shows the DSC 0.94 and 0.92 for the femur and tibia, respectively.

Balsiger *et al*. [14] developed a method using random forest (RF) and semantic context forests learning models to

automatically segment distal femur bone. To test/validate this methodology, 19 datasets were taken, out of which 10 were manually labelled. DSC calculated for the distal femur (DSC – 0.92) shows a good agreement between manually labelled segmentation and automatically developed method.

Shan *et al*. [18] provided a two-step technique of bone segmentation and elastic tissue deformation to rectify faults made in their earlier work. From the T1 and T2* pictures, the images of the femur and tibia are automatically segmented and extracted. When attempting to find a solution to a problem involving continuous convex optimization, geometric and shape information is taken into account. The incorporation of essential information that is appearance-based assists in the optimization process. If you skip the phase when the forms are aligned, you'll have better success segmenting the data. Because of the unique physical characteristics of the tissues that make up the knee, standard registration poses a challenge to ensure that the knee is properly aligned (bone, muscle, *etc*.). Because of this, the author devised a novel approach to re-aligning one's bones using an elastic deformation model, and the stringent enforcement of similarity transforms.

Using a unique approach that was proposed by Ratzlaff *et al*. [19], subchondral bone marrow lesions that were discovered by MRI in patients with knee osteoarthritis may be measured. This study's primary objective is to assess the reliability and validity of an automated quantitative method for determining the presence of osteoarthritis-related bone marrow lesions (BMLs) in the femur and tibia of study participants. Whole-Organ Magnetic Resonance Imaging Score (WORMS) scoring was used to validate the BML volume criterion. The Western Ontario and McMaster University OA Index weight-bearing pain questions were also used by the researchers to investigate the relationship between BML volume in the tibiae and femurs of the knee.

The proximal femur extraction from MR images and segmented with the help of neural networks was the subject of investigation carried out by Deniz *et al*. [20]. This study aims to develop a method for the automated segmentation of the proximal femur based on deep convolutional neural networks (CNNs). After ensuring that every participant was provided with enough information and given the opportunity to provide their informed permission, the university's institutional review board approved the research project.

In the future work done by Deniz *et al*., more than eighty-six individuals' lower leg volumetric structural images were manually segmented by a medical practitioner. To evaluate and compare the segmentation capabilities of two distinct CNN architectures, each network was trained using a unique combination of the starting feature map count, layer count, and dilation rate. The lower femur was segmented using CNN, and the results produced were excellent in terms of accuracy. The dice similarity score was 0.950.02, while the values for precision and recall were also 0.95.02. Because of the high level of segmentation accuracy that CNNs possess, it is possible that they might be useful in the treatment of osteoporosis.

Two separate CNN architectures, each with a different number of initial feature maps and layers, are put through four-fold cross-validation to compare their results to the hand segmentations that serve as the gold standard. A 3D convolution-based CNN architecture performs better when segmenting the proximal femur than a 2D CNN. This design produced dice similarity scores of 0.94±0.05 with precision = 0.95±0.02 and recall = 0.94±0.08 for the latter. Due to the exceptional segmentation accuracy that CNNs provide, it is possible that they might facilitate the incorporation of structural MRI assessments of bone quality into clinical practice for osteoporosis therapy. Improving knee joint tissue segmentation efficiency and accuracy is possible using techniques such as deep convolutional neural networks (DCNN). 3D fully connected conditional random fields (CRF) and simplex deformable modelling [20].

A new transparent computer-aided diagnosis method based on Knee osteoarthritis (OA) severity was automatically scored using the Deep Siamese Convolutional Neural Network created by Tiulpin *et al*. [24] using Kellgren-Lawrence (KL) grading technique. The author developed and assessed a method based on findings from the Osteoarthritis Initiative and the Multicenter Osteoarthritis Study, funded by the Osteoarthritis Initiative. Compared to the annotations provided by a panel of clinical experts, the recommended technique has a quadratic Kappa coefficient of 0.83 and an average multi-class accuracy of 66.71 percent. In this particular investigation, it was shown that the AUC for radiological OA was 0.93. The radiological properties that affect network decision-making are highlighted using a probability distribution of classes.

Gandhamal *et al*. [33] presented their work on subchondral bone segmentation by utilizing MR scans of the knee. The results of this work have made it feasible to independently segment subchondral bone from MR images of the knee. During this research, MR images of the knees were enhanced using gray-level S-curve processing, automated seed point recognition, and three-dimensional multiple-edge overlap. As can be seen in the picture, level-set evolution is used to first extract bone sections and then to find and patch leaks along bone border regions using boundary displacement. This process is repeated until all leaks along bone border regions have been fixed. The sensitivities and specificities of the suggested method, as well as the DSC, average surface distance (AvgD), and root mean square surface distance (RMSSD), were evaluated in comparison to real-world settings (RMSD). All segmentation findings were acquired with confidence intervals of 95 percent utilizing a total of eight separate datasets. An average sensitivity (91.14%), specificity (99.12%) and DSC (90.28%) with 95% confidence interval (CI) in the range 89.74 – 92.54%, 98.93 – 99.31% and 88.68 – 91.88% respectively is achieved for the femur bone segmentation. Because of this study's reliability and robustness, the suggested methodology can be used for large-scale and long-term research into knee OA in clinical settings.

Chen *et al*. [34] proposed a knee bone segmentation method based on a 3D Deep Neural Network Using Adversarial Loss for Prior Shape Constraint. To enlarge the contextual information and incorporate prior shape constraints, a three-dimensional (3D) deep neural network with adversarial

loss was proposed to automatically segment the knee bone in a resampled image volume. A restoration network was proposed to improve bone segmentation accuracy further by restoring bone segmentation to its original resolution. Regarding the SKI10 validation dataset, the proposed method received a score greater than 76. This method proved robust in extracting bone and cartilage masks from the MRI dataset, even for the pathological case.

Fast and accurate segmentation of knee bone and cartilage on MRI images is becoming increasingly important in the orthopedic area, as the segmentation is an essential prerequisite step to a patient-specific diagnosis, optimizing implant design and preoperative and intraoperative planning. However, manual segmentation is time-intensive and subjected to inter- and intra-observer variations. Various semi-automatic and fully automatic methods have been developed to segment knee bones accurately. The application of deep learning-based approaches for knee bone segmentation provides promising results. Researchers have proposed various deep learning-based networks, giving more accurate results than manual and semi-automated methods.

Jiang *et al*. developed their combined segmentation strategy. They use a multiphase Chan-Vese model that has been upgraded. According to the investigation's findings, a multiphase model of the knee joint was used in this study. To begin, the author introduces a new energy function based on the anatomical structures and intensity distributions of knee joints in the horizontal section, with the goal of keeping the evolving curves in the same relative location as the initial ones. This metric correct segmentation errors and ensures segmentation results are accurate. Then, another interior energy term is introduced to keep the evolving curves close to the signed distance functions. Re-initialization, which is time-consuming and required in the traditional Chan-Vese model, is never required in this manner, and segmentation convergence becomes rapid and smooth. The results of segmenting knee joints in MRI and CT validate the approach's effectiveness and efficiency compared to the original multiphase Chan-Vese model.

2.2. Cartilage Segmentation & Quantification of Morphoslogy

Because of its unpredictable form, bulk (the typical thickness of cartilage is around 4 millimeters), and connections with other tissues [35, 36], AC is difficult to segment. The studies that have been published after 2010 and are included in Table **2** are those that focus on the development of computational algorithms for segmenting articular cartilage from knee MR data. In addition, the Medical Image Computing and Computer Assisted Intervention Society (also known as The MICCAI Society) initiated a massive project in 2010 with the goal of segmenting articular cartilage and bone from MR images of the knee, which was followed by the extension of submissions of segmentation results through an internet service [37].

Table 2. Automatic segmentation of AC: Existing studies (After the year 2010).

Study/Refs.	MR Pulse Sequence	Technique Used	Sensitivity (%)	Specificity (%)	DSC
Ambellan *et al*. 2018 [25]	SKI10, OAI Imorphics and OAI ZIB datasets	3D Statistical Shape Models (SSMs), as well as 2D and 3D CNNs	-	-	DSC is 98.5% for FB, 98.5% for TB, 89.9% for FC, and 85.6% for TC
Lee *et al*. 2011 [38]	Double-Echo Steady-State (DESS)	Optimization of Local Shape and Appearance	NR	NR	Femur- 0.77 Tibia- 0.81
Liang *et al*. 2012 [39]	SPGR	KNN Classification	Femur- 80.7 Tibia- 83.3	Femur- 0.99 Tibia- 0.99	Femur- 0.75 Tibia- 0.81
	T1 weighted magnetic resonance (MR) knee images	multi-atlas-based method to automatically segment the femoral and tibial cartilage	-	-	femoral = 75.2% and tibial cartilage = 81.7%
Zhang, Lu *et al*. 2013 [40]	FS SPGR, FIESTA, IDEAL GRE Water, IDEAL GRE Water Fat	Multi-contrast MR and Classification	Femur-82.6 Tibia-86.0	Femur -99.6 Tibia-99.5	Femur- 0.86 Tibia- 0.88
Lee 2013 [41]	GRE T1-weighted with FS	Multiple-Atlas and Locally Weighted Vote (LWV)	Tibia-53.0 Femur-57.5	Femur -99.9 Tibia-99.9	Femur -0.67 Tibia- 0.53
Shan, Zach *et al*. 2014 [42]	T1-weighted (3D SPGR)	Multi-atlas and Multi-level	-	-	Femur-0.856 Tibia-0.859
Pang, Li *et al*. 2015) [43]	T2-Weighted and Fat Suppression	Pattern Recognition with Bayesian Classifiers	-	-	Femur-0.804 Tibia-0.726 Patella-0.700
Öztürk and Albayrak 2016 [44]	Double-Echo Steady-State (DESS)	Voxel-Classification driven Region-Growing	Femur- 79.9 Tibia-84.0 Patella-71.5	Femur- 99.8 Tibia- 99.9 Patella-99.9	Femur- 0.826 Tibia- 0.831 Patella-0.726
Falicia 2017 [45]	3DT1 VIBE WE	2DUNetcascade- deep learning	Femur -0.782	Femur -0.998	Femur DSC- 0.717
Norman *et al*. 2018 [46]	Double-Echo Steady-State (DESS)	2D U-Net Convolutional Neural Networks	-	-	Cartilage 0.770 -0.878

(Table 2) contd.....

Study/Refs.	MR Pulse Sequence	Technique Used	Sensitivity (%)	Specificity (%)	DSC
Dodin *et al*. 2012 [47]	T1/T2*-weighted gradient echo (DESS) and a water-sensitive intermediate-weighted turbo spin echo (IW-TSE)	Selection of bright, structured areas corresponding to BMLs, geometric filtering of unrelated structures, segmentation of the BML, and quantification of BML proportion within bone regions.	-	-	-
Ahn *et al*. 2016 [48]	3-D DESS WE image series	Initial contour and level-set method with modified localizing region-based active contours	Femoral cartilage -90.6%, Tibial cartilage- 87.5%, Patellar cartilage- 90.2	Femoral cartilage -99.7%, Tibial cartilage- 99.9%, Patellar cartilage- 99.8	Femoral 87.1, patellar 84.8 and tibial cartilage 81.7
Brui *et al*. 2018 [49]	1.5T using a VIBE sequence	Genuine CNN for the wrist cartilage segmentation	-	-	0.81±0.11
Liu *et al*. 2018 [50]	Single sagittal fat-suppressed T2-weighted fast spin-echo MRI sequence	A convolutional encoder-decoder network for segmenting cartilage and bone followed by a second CNN classification network to detect structural abnormalities within the segmented cartilage tissue.	-	-	Femur - 0.96 ± 0.02 tibia - 0.95 ± 0.03 femoral cartilage - 0.81 ± 0.04, tibial cartilage - 0.82 ± 0.04 .
Liu *et al*. 2018 [51]	Sagittal T1-weighted spoiled gradient-echo (SPGR) knee images	Combine a semantic segmentation CNN and 3D simplex deformable modeling	-	-	-
Liu *et al*. 2018 [52]	PD-FSE dataset and T2-FSE dataset	Cycle-consistent generative adversarial network	-	-	Femur - 0.97, Tibia - 0.93, Femoral Cartilage - 0.65, Tibial Cartilage - 0.64
Kashyap *et al*. 2019 [53]	All subjects were scanned using the DESS protocol	Just-enough interaction (JEI)	-	-	-
Bonaretti *et al*. 2019 [54]	T2-weighted images	Pioneer framework	-	-	DSC for OAI1 dataset - 0.81
Kashyap *et al*. 2019 [55]	All subjects were scanned using the DESS protocol	Hierarchical Classifiers and Just Enough Interaction based Learning	-	-	-
Kashyap *et al*. 2019 [56]	Double echo steady state (DESS) MRIs	Learning-Based Cost Functions for 3D and 4D Multi-Surface	-	-	-
Jurgen Fripp *et al*. 2010 [57]	T1 weighted FS SPGR images, weDESS, and MEDIC MR images.	Three-dimensional active shape model	-	-	DSC of (0.83, 0.83, 0.85) for the (patellar, tibial, femoral) cartilages
Pierre Dodin *et al*. 2010 [58]	3T scanner and a knee coil and the exam consisted of a double echo steady state (DESS) sequence	Segmentation algorithm for human osteoarthritic knee cartilage volume quantification from MR images, taking into account the aforementioned problems	-	-	(DSC) for the global knee ($r = 0.96$, $p < 0.0001$, and median DSC = 0.84), for the femur ($r = 0.95$, $p < 0.0001$, and median DSC = 0.85), and the tibia ($r = 0.83$, $p < 0.0001$, and median DSC = 0.84)
S. Shah 2010 [59]	Sagittal 3D MR images were acquired at 1.5T using a phased array surface coil with an in-plane resolution	Bezier splines and Canny edge detection	-	-	-
M. Swamy *et al*. 2010 [60]	A water excitation double echo steady-state (DESS) imaging protocol with sagittal slices at 3.0T	Precise cartilage reconstruction, visualization and quantification are carried out in the detection and treatment of OA.	-	-	-
Long *et al*. 2010 [61]	MRI scans	Integrate active contour models (Snake) with artificial neural network	-	-	-

(Table 2) contd.....

Study/Refs.	MR Pulse Sequence	Technique Used	Sensitivity (%)	Specificity (%)	DSC
Williams *et al*. 2010 [62]	A fat-suppressed -weighted 3-D gradient echo sequence for visualization of the hyaline cartilage, and a -weighted sequence	Anatomically corresponded regional analysis of cartilage (ACRAC)	-	-	-
Yin *et al*. 2010 [63]	A sagittal 3-D dual-echo steady state (DESS) sequence with water-excitation	Algorithmic incorporation of multiple spatial inter-relationships in a single n-dimensional graph, followed by graph optimization that yields a globally optimal solution	-	-	DSC values of femoral = 0.84, tibial =0.80 and patellar cartilage regions = 0.80
Peña *et al*. 2011 [64]	3D DESS MRI images	Precisely characterize and measure cartilage changes in volume, thickness and shape changes in natural OA progression	-	-	-
Zhang *et al*. 2011 [65]	A 3.0T magnet scanner with multiple MR sequences, including FS SPGR, FIESTA, and IDEAL GRE.	Cartilage segmentation with multi-contrast MR images based on pixel classification	0.909±0.114	0.997±0.002	0.913±0.090
Marstal *et al*. 2011 [67]	A FLASH Gradient Echo (GR) sequence	Semi-automatic and requires a minimal amount of manual intervention	Tibial = 0.853 ± 0.093,femoral cartilages = 0.831 ± 0.095	Tibial = 0.999,femoral cartilages = 0.999 ± 0.001	Tibial = 0.800 ± 0.106 ,femoral cartilages = 0.777 ± 0.054
Tran *et al*. 2012 [68]	Real magnitude MR images of the human knee	The least squares approach is employed. Then, a total variation noise removal algorithm using an iterative scheme is applied. After that, the vector field convolution active contour method.	-	-	-
Tamez-Pena *et al*. 2012 [69]	Vivo 3-D dual echo steady state images.	Multiatlas automated knee segmentation method and apply it to the OAI pilot scan–rescan images	-	-	Femoral = 0.88 and tibial cartilage = 0.84
Kashyap *et al*. 2013 [70]	MR field strength of 1.5 T and the rest 3 T and 1 T	A modified Layered Optimal Graph Image Segmentation of Multiple Objects and Surfaces (LOGISMOS)	-	-	-
Prasoon *et al*. 2013 [71]	(MR) images from the Osteoarthritis Initiative (OAI) database	Two-stage classifier for segmenting tibial cartilage in knee MRI scans combining nearest neighbor classification and support vector machines	80.8236%	98.0760%	0.8115
Prasoon *et al*. 2013 [72]	Specialized extremity MRI scanner	A novel system for voxel classification integrating three 2D CNNs, which have a one-to-one association with the xy, yz and zx planes of 3D images, respectively	81.92%	99.97%	0.8249
Shan *et al*. 2013 [73]	Pfizer Longitudinal Dataset (PLS-A9001140) which contains T1-weighted (3D SPGR) images	A novel general spatiotemporal three-label segmentation method	84.2% (6.3%)	99.8% (0.07%)	81.8% (3.5%)
Gan *et al*. 2014 [74]	Dual echo steady state (DESS) MR knee images with water excitation	Random walks to facilitate the segmentation process.	0.86	0.99	0.82
Kubicek *et al*. 2014 [75]	Proton-dense sequence with fat suppression and gradient spin-echo sequence	Detection of local extremes in the histogram and uses a membership function to allocate each image density into an output set	-	-	-
Gan *et al*. 2018 [76]	Osteoarthritis Initiative (OAI) and Multicenter Osteoarthritis Study (MOST)	A binary seeds auto-generation model to reduce the reliance on manually crafted priori information in deep learning	0.96±0.051	0.997±0.0019.	Reproducibility = 0.92±0.051

(Table 2) contd.....

Study/Refs.	MR Pulse Sequence	Technique Used	Sensitivity (%)	Specificity (%)	DSC
Revathi *et al*. 2018 [77]	MRI sequences are the most frequently used for cartilage volume assessment on 1.5T apparatus gradient echo sequences	There are two processes of segmentation here, one after the other, the number of morphological operations at the final segmentation process.	-	-	-
Viken 2020 [78]	Real arthroscopic images from surgeries are considered.	Used MultiResUnet architecture for accurate segmentation. Classification of multifractal features using neural networks is also shown to perform as well.	0.7±0.014	0.8±0.012	Mean Pixel Acc. 0.9±0.006
Xue *et al*. 2021 [79]	Cones-T1, Cones-AdiabT1, Cones-T2*, and MMF were measured using a series of 3D UTE cone sequences. Cones-T1 imaging was performed using actual flip angle imaging, followed by variable flip angle (AFI-VFA) imaging with four different flip angles (5°, 10°, 20°, and 30°).	3D ultrashort echo time (UTE) cones MR imaging with deep convolutional neural networks	-	-	Mean Dice scores were 0.81 ± 0.11 for Rad1 *vs*. CNN1 and 0.82 ± 0.08 for Rad2 *vs*. CNN2, respectively.
Kessler *et al*. 2022 [80]	2-weighted images from the OAI dataset were registered to the DESS images	The 3D cartilage surface mapping (3D-CaSM) method, a surface-based analysis of cartilage morphology (thickness) and composition (T2), was performed using both manual and network-generated segmentations from OAI ZIB testing images.	-	-	Cartilage thickness measurements range between -0.12 to 0.33 [-0.28, 0.96] mm with 2D U-Net and 0.07 to 0.14 [-0.14, 0.39] mm with 3D U-Net. For T2, the mean bias [95% limits of agreement] ranged between -0.16 to 1.32 [-4.71, 4.83] ms
Yang M *et al*. 2022 [81]	Siemens 3T Trio scanner using the 3D sagittal double-echo steady state (DESS) sequence with the same coil model and acquisition parameter settings	Generative adversarial networks with transfer learning	-	-	Dice coefficient of 0.819, an HD95 of 1.463 mm, and an ASSD of 0.350 mm

The difficulty of correctly and completely automating the segmentation of articular cartilage using different pattern recognition algorithms have been the subject of much research that has sought to solve this problem.

Researchers have proposed various automatic segmentation algorithms, a selection of which has been summarized in the sections that came before it. Different classifiers have been used to differentiate the AC voxel from the voxels that represent other tissues or the backdrop, and deformation models and graph models were utilized to construct these methods. Certain researchers have created more advanced methods, including multi-nuclei, multi-contrasts, multi-contrasts, multi-levels, and multi-object-based algorithms, in order to automatically differentiate AC pictures from MR images. Even though many automated articular segmentation procedures can be found in the literature, there is still a need for research in this area. As was said before, many existing systems have various flaws. A great quantity of learning data is necessary for most of the techniques, and just a little change in the data may have the potential to have a big influence on the outcomes that may be achieved. Even making little adjustments to the data requires an equivalent time commitment in the beginning stages. Researchers could make a substantial contribution to this field by inventing efficient methods in terms of both time and computing while retaining a high level of sensitivity, selectivity, and dynamic range (DSC).

Osteoarthritis patients must have their bone marrow lesions (BMLs) identified and quantified since these lesions are the root cause of increased pain and deterioration of cartilage. In this investigation, MRI was used, and two different sequences were performed: a T1/T2*-weighted gradient echo and a water-sensitive intermediate-weighted turbo spin echo (DESS). The study aimed to create a quantitative BML evaluation technique for human knee OA (IW-TSE).

A multi-atlas- based technique is presented by L. Shan *et al*. [39] for segmenting femoral and tibial cartilage from T1 scans. The segmentation outcomes could be determined by using a variety of atlases for the registration process and Bayesian approaches. An application of the probabilistic k-closest neighbor classification was used to obtain the cartilage likelihoods. It was shown that the femoral and tibial cartilage in this osteoarthritis dataset, comprised of 18 MR images of the knee and manually segmented by experts, was properly segmented. MRI scans have made it feasible to detect osteoarthritis in its earliest stages and conduct assessments on patients suffering from the condition (OA). The rate of cartilage loss in the individual plates may vary significantly

from one another. The segmentation of cartilage plates and accurate delineation is no longer attainable by the use of automated techniques.

Automatic segmentation of knee joint cartilage in high-field magnetic resonance images was accomplished by C. Oztürk *et al*. [44] by using an enhanced region-growing technique that included proximity-correlated subsampling. Using voxel classification methods, magnetic resonance imaging (MR) can unequivocally identify degradable anatomical components such as cartilage. It requires a significant amount of processing power to segment high-field MR images using voxel classification. The knee joint's femoral, tibial, and patellar cartilage compartments were autonomously partitioned using a region growth algorithm driven by the voxel classification, as stated by the MR images provided by the Osteoarthritis Initiative. By removing background voxels from the training MR images and selecting just a small sample of important attributes, researchers were able to reduce the amount of computational complexity associated with the classification. This was accomplished considering that some systems have restricted memory and processing capability.

Dodin *et al*. [47] worked on transferring bone and cartilage objects from previously published automated technology to the DESS sequence. After that, they went on to quantify BMLs using a four-stage process, which included the following steps: selection of bright, structured areas that correspond to BMLs; geometric filtering of unrelated structures; segmentation of the BML; and quantification of the BML proportion with IW-TSE sequences. The reliability of BML manual segmentation (DESS and IW-TSE) was tested by applying intra-class correlations on 154 OA patients from the Osteoarthritis Initiative (OAI) cohort (available datasets) (ICC). The newly found automatic algorithms for BML localization and geometric extent were compared with manual segmentation (DSC) using ICC and Dice similarity coefficients. In the last step, a comparison was made between the incidence and proportion of BML in the DESS and IW-TSE sequences.

Lee *et al*. [38] provided a totally automated technique for analysing 3-D MR data. This system included bone segmentation, BCI classification, and knee cartilage segmentation. Binary classification is a method proposed by authors for the BCI. This method depends on binary location and local appearance classifiers for bone segmentation. This work significantly contributes to the area of cartilage segmentation by using locally produced and optimized Markov random fields (MRFs).

In order to determine the region and border potentials of the MRFs, training pictures unique to each local patch are used in the calculation. The local image characteristics are employed in this tactic to combine the local signals for the object's form and look. In order to investigate theories about the impact that exercise has on cognitive function, an MR imaging dataset was used. This dataset consisted of the baseline and follow-up scans taken two years later of 10 different people. Comparisons of the proposed method's qualitative and quantitative findings with other semi-automatic segmentation options demonstrate the technique's potential for therapeutic applications.

Adaptive force function and template-based segmentation of the knee MRI using the results of Ahn *et al*. [48] osteoarthritis initiative article. Researchers have developed a ground-breaking knee cartilage segmentation method. Compared to the traditional procedures, the DSC approach led to considerable improvements in the patient's patellar, femoral, and tibial cartilage. In a study involving 10 individuals, the dice similarity coefficients were 87.1 percent, 84.8 percent, and 81.7 percent.

Research on the deep learning-based, fully automated segmentation of wrist cartilage in MR images was carried out by Brui *et al*. [49]. Researchers developed, tested, and validated an autonomous system based on deep learning to segment the cartilage in the wrist joint using magnetic resonance imaging (MRI). The participants in the research were all suffering from issues related to the joints in their wrists. It was possible to acquire a total of 20 3D MRI datasets at 1.5T by using a VIBE sequence. Convolutional neural networks (CNNs) were trained and evaluated using coronal slices of wrist cartilage as its data source. A dataset consisting of 20 central coronal slices was segmented three times and twice by the same observer to conduct an inter- and intra-observer analysis on wrist cartilage.

This study used concordance and Srensen–Dice similarities to compare CNN and hand segmentations. Osteoarthritis, often known as OA, is a debilitating condition affecting over one-third of adults over 60.

Liu *et al*. [50] worked on “Deep Learning Approach for Evaluating Knee MR Images: This work aims to determine the feasibility of using a deep learning approach to detect cartilage lesions in MR images. Fat-suppressed T2-weighted, fast spin-echo MRI data sets of the knee of 175 patients with knee pain were retrospectively analysed. The reference standard for training the CNN classification was the interpretation provided by a musculoskeletal radiologist of the presence or absence of a cartilage lesion.

A 3D deformable approach was developed by Liu *et al*. [51] for determining tissue segmentation in musculoskeletal magnetic resonance imaging. The segmentation process is broken down and analyzed using unlabeled MR images and a neural network that combines adversarial and segmentation convolutional layers (CNN).

The assistance of adversarial and segmentation networks was used to construct segmentation pipelines. The fundamental method to translate unpaired pictures was called cycle-consistent generative adversarial network (CycleGAN). The performance of semantic segmentation was bolstered by including a mixed segmentation network inside the adversarial network. In order to segment bone and cartilage, the fully automated segmentation approach known as SUSAN was put through its paces on two clinical knees MR imaging datasets. SUSAN used pictures and annotated masks from a publically accessible online collection of knee MR images. The segmentation outcomes were analysed and compared using two different registration methods and two different supervised U-Net segmentation strategies. In order to determine the degree of variation present in quantitative measures, the Wilcoxon signed-rank test was used for the data collected. Magnetic Resonance Imaging of the Skeletal and Musculoskeletal

Systems for Tissue Segmentation Imagine a deep convolutional neural network working with a 3D deformable neural network.

Semantic dissection as a basis for segmentation CNN and 3D simplex deformable modelling was used to develop a method for completely automatic segmentation [52]. The segmentation technique was supported by SegNet, a CNN method for multi-class tissue classification at high-resolution pixels. This method served as the strategy's backbone. In order to keep its general form and a smooth surface ideal for the musculoskeletal system, it was required to adapt the output of SegNet using 3D simplex deformable modelling. The fully automated segmentation technique was compared to other state-of-the-art segmentation algorithms using a knee MRI dataset accessible to the public.

The knee joint is particularly notable for its degree of both intricacy and sensitivity. Articulations are a common factor in the development of knee injuries and damage. Those who suffer from knee osteoarthritis may find that the accompanying pain and restrictions incapacitate them to the point that they cannot function normally (OA). Two types of cartilage may be found in joints: articular cartilage and synovial cartilage. Pain is caused when cartilage deteriorates and is worn away due to osteoarthritis (OA).

An automatic layered optimum graph segmentation of numerous objects and surfaces (LOGISMOS) is integrated into an instant rectification phase as part of the interactive approach known as just-enough interaction (JEI), which was developed by Kashyap *et al*. [53]. The JEI user input did not influence the boundary surfaces of the bones and cartilages in the knee MRI after the LOGISMOS segmentation was performed. After adjusting the local costs of the underlying network nodes, the graph is re-optimized to get globally optimum results that have been rectified.

Clear musculoskeletal imaging is necessary for the diagnosis of osteoarthritis (OA). OA is a chronic disease that wears away at the cartilage in the femoral knee and has the potential to cause disability. Researchers have developed methodologies that are both transparent and capable of being replicated. In order to design and operate the majority of these algorithms, advanced programming abilities are necessary.

However, the use of methods that are both open and able to be replicated is very necessary in order to hasten the discovery and conclusion of new facts and ideas. Using MR images, S. Bonaretti *et al*. [54] provide Pioneer, a platform that enables open and repeatable research into femoral knee cartilage. This Python-based program, which uses Jupyter Notebooks to provide users with a graphical user interface, is governed by the GNU GPLv3 open-source license. Three components comprise the whole: Image preprocessing was used to normalize the spatial and intensity features prior to doing intersubjective, multimodal, and longitudinal research on femoral knee cartilage. Segmentation and analysis of the femoral knee cartilage were then done. Each module comes with a selection of Jupyter notebooks, which may be used to simulate various computing environments. Researchers that employ transparent image analysis to investigate the femoral knee cartilage have found that Pioneer's simplicity of installation and usage and its publishing and sharing options have been of significant use to their work. Because of its modular architecture, Pioneer makes it simple to expand and compare different algorithms.

Kashyap *et al*. [55] assert that they have created a completely automated learning-based method for segmenting osteoarthritic knee cartilage (OA). The approach utilizes random forests across the many levels of its hierarchical structure. On the other hand, the feature set used by RF classifiers is the output probability map generated by a neighborhood approximation forest (NAF). The best graph segmentation of many objects and surfaces should use hierarchical probabilities as cost functions (LOGISMOS). The author of this research details it and illustrates how to build a large number of training instances quickly and consistently *via* a unique post-processing interface (JEI). For the purposes of training, a total of 53 knee datasets were used, and for the purposes of testing, 15 knee datasets were utilized. Using a double echo steady state (DESS) technique, an MRI was used to get every picture from the OAI database. Compared to the traditional gradient-based cost functions, the learning-based cost function significantly reduced the number of segmentation mistakes (p less than 0.05).

The Osteoarthritis Initiative contributed to the data used in Kashyap *et al*. [56] presentation on learning-based cost functions for 3D and 4D multi-surface multi-object segmentation of knee MRI. Using a unique hierarchical collection of RF classifiers, researchers have devised a completely automated system for analyzing osteoarthritis (OA). For layered optimum graph image segmentation of multiple objects and surfaces, LOGISMOS uses a neighborhood approximation forest to give context for the second-level RF classifier.

Researchers have developed a machine-learning classifier that considers both the 3D spatial environment and the passage of time. This classifier also incorporates local features and outputs location-specific costs. After a year, at least one-third of the 54 patients evaluated with 4D LOGISMOS showed a significant reduction in the number of segmentation mistakes (p0.001). Researchers examined the same group of 54 patients five times over the course of one year.

Fripp *et al*. [57] used magnetic resonance images of the knee to automatically segment the articular cartilages and then statistically analyzed the results of their work. The authors provide a segmentation technique based on MR images of healthy knees that differentiates cartilage and bone consistently and automatically. The segmentation of bone and cartilage is accomplished by using a 3D active shape model that combines patient-specific tissue estimations with deformable models that incorporate the thickness fluctuation of the cartilage as described in this study. This model is used to carry out the segmentation process. MR images were used so that the accuracy of examining gradient recall datasets that have had their fat content reduced could be evaluated. As a method of comparison, they used non-rigid registration in conjunction with tissue classification (B-spline-based free-form deformation).

Dodin *et al*. [58] devised a way to evaluate the amount of human knee cartilage using MRI data and an artificial segmentation approach. In order to construct a parametric bone–cartilage contact surface on the femur and tibia, it was essential to segment the three-dimensional data from the MRI. In order to complete the first step, there was a need to reduce the resolution of the MR images that cover the area close to where the bone surface meets the bone. In order to recognize cartilage as bright and uniform, filtering procedures are used for a second time. Due to the fact that this procedure does not include any soft tissues, the outermost border of the cartilage may become visible. Third, using Bayesian judgment criteria, it is possible to automatically distinguish cartilage and synovial fluid from one another. Ultimately, the technology created was used to determine a person's cartilage volume and how it varies over their lifetime. The novel and automated method described in this article may assess knee cartilage volume with pinpoint accuracy. These evaluations are intended for clinical research purposes.

Shah *et al*. [59] presented a more straightforward method for estimating and visualizing MRI cartilage of the knee in their study. One of the most important objectives of this research is to simplify the description of knee cartilage by using segmentation, analysis, and visualization techniques. This research uses a technique for semi-automatic segmentation based on Bezier splines and intelligent edge detection. When using an anisotropic diffusion technique, it is possible to discern the borders of the cartilage in the pictures quite clearly. A shape-based interpolation technique is applied to segmented cartilage to get isotropic voxels and then employed in a basic manner. MRI registration involves making artificial connections between points located on various slices of the brain. After the thickness and volume of the cartilage have been determined, an evaluation may be performed. Visualizing articular cartilage offers a different approach to the traditional way of measuring it.

According to the findings of this study by M. Holi *et al*. [60], cartilage is present in both normal and osteoarthritic knee joints. This cartilage may be seen and quantified. In the course of this research, image processing methods were used for the examination of MRI scans of the knee. Techniques such as Canny edge detection and histogram averaging are used in order to accomplish this goal. The femur, the tibia, and the menisci cartilages may all be segmented with this approach. Using this technique, the cartilage in the knee may be seen. The thickness of the cartilage in individuals with normal conditions and OA is measured. The findings might be used to get a deeper comprehension of the processes that lead to the development of OA and to better direct treatment decisions pertaining to this illness.

Long *et al*. [61] conducted research on the use of artificial neural networks in the process of cartilage segmentation. Magnetic resonance imaging, sometimes known as MRI, provides the best noninvasive image of articular cartilage. This imaging technique examines the structure, biochemistry, and function of cartilage. This study tries to tackle the difficult problem of automatically calculating cartilage amounts. Initially, a clustered segmentation method is built using algorithms based on common segmentation techniques, such as thresholding and poly fitting, and calculating the average weight. This is done in order to create the segmentation method. An artificial neural network (ANN) has been used to refine further the method to address the nonlinearity and inexplicable MRI image anomalies. The needed results may be obtained by combining active contour models with this ANN (Snake). An example based on computation is offered to validate the findings and explain the methodology developed.

Williams *et al*. [62] gave a presentation titled "Statistical Shape Modelling of the Bone: The Analytic Study of Cartilage between Asymptomatic as well as Osteoarthritic Knees." ACRAC is a unique method for the anatomically-correlated globalized context of cartilage, which may be used to analyze the morphology of knee cartilage in anatomically corresponding focal regions defined on the surface of the bone. Researchers divided the bone fragments in the knees of 19 healthy women volunteers after doing 3-D knee scans on them. In order to generate statistical shape modelling (SSMs) with a minimal description length (MDL), the segmented bone surfaces were employed. These models supplied mean bone shapes and a dense collection of anatomically matching places on each bone. The precision of such SSMs was evaluated using repeat photos provided by a selection of the participants.

Yin *et al*. [63] developed an innovative approach called layered optimal graph image segmentation of multiple objects and surfaces (LOGISMOS) that can concurrently segment many interacting surfaces corresponding to several different objects that interact with one another. The first step in the process is the algorithmic incorporation of multi-spatial interrelationships into a single n-dimensional graph, which is subsequently optimized to produce a global solution. In order to demonstrate the applicability and effectiveness of the LOGISMOS approach, bone and cartilage from a human knee joint have been segmented. Despite being trained on a small set of nine photographs, this system performed quite well after evaluation.

Tamez-Peña *et al*. [64] provided data from the osteoarthritis project paper on the automated segmentation and quantification of knee features using an atlas-based approach. Tamez-Peña *et al*. Their study provides an unsupervised method for segmenting 3D DESS MRI images of the human knee. This method was reported in their paper. Five MRI knees that were manually segmented make up the reference atlases used in automatically segmenting subsequent MRI images. The segmentation of the knee is produced by taking the average of the results of the other five segments. Images from the Osteoarthritis Initiative (OAI) DESS sequence were used to conduct the evaluation.

Zhang *et al*. [65] proposed a novel method for cartilage segmentation that uses multi-contrast MR images and pixel classification to get precise and automated results. When it comes to cartilage segmentation, all that is required are trained classifiers such as support vector machines (SVMs) or k-nearest neighbors. On the other hand, this particular set of guidelines does not consider any geographical information.

Authors employ loopy belief propagation inference to

determine which label arrangement is the most effective. The characteristics employed may be categorized into local picture structure features and geometrical information-based features. Experiments have demonstrated that the combined features are superior to the two types of individual features as well as the conventional frameworks that are purely based on SVM or DRF for cartilage segmentation.

Marstal *et al*. [67] asserted that a novel technique had been devised for segmenting the osteoarthritic cartilage in the knee in MRI images. Using this modern approach, magnetic resonance imaging may segment cartilage from the knee. There must be some degree of manual involvement, although it may be rather light. The Kellgren-Lawrence grading method for knee osteoarthritis assesses the prescribed treatment using scans from fifty. The segmentation of MR images is essential in automatically diagnosing medical conditions. Such photos get distorted due to the Rician noise and the fuzzy edges.

The combination of methods described in Tran *et al*. [68] made it simpler to automatically separate articular cartilage from noisy MR images. As illustrated in the work of T. Pena *et al*. [69], it is feasible to avoid falling into local optimization traps by defining the beginning contour in a different method for each section of the knee. This will allow the knee to be optimized more globally. This paper demonstrates the automated segmentation of knee cartilage and bone using *in vivo* three-dimensional dual-echo steady-state images.

The longitudinal scans of healthy controls and patients with knee osteoarthritis (OA) that were performed twice at each visit were included in the MRI datasets that were collected as part of the Osteoarthritis Initiative (OAI) pilot study and were used to compile the MRI datasets (baseline, 24 months). Initially, human professionals were responsible for segmenting six different MRI sequences. Five of the six sets of results generated by a multi-atlas segmentation approach could serve as reference atlases. In order to determine the curvature of the subchondral bone plate and the volume, surface area, and thickness of the articular cartilage in the knee, exact segmentations of the knee were required.

Kashyap *et al*. [70] devised a method for autonomous segmenting and defining cartilage plates. As a result of this, the author has made efforts to enhance the accuracy of the segmentation of a wide variety of objects and surfaces by using layered optimal graph image segmentation (LOGISMOS). This method was evaluated by applying it to sixty different data sets provided by the MICCAI segmentation competition in 2010. There is a mean value as well as a standard deviation associated with the surface location inaccuracies of each cartilage plate region.

Prasoon *et al*. [71] successfully segmented femoral cartilage in knee MRI images using two voxel categorization steps. Even if a classifier does not scale well with the number of training samples, it is still possible to incorporate effective classifiers into tasks requiring a significant quantity of data for training by using multiple classification stages and exploiting the imbalance across class populations. This is the case even if the task requires a great deal of data. Therefore, in order to segment knee cartilage in photographs of knees, we constructed a two-stage classifier by combining the techniques of nearest neighbor classification and support vector machines (SVM). Using this method, individual segments of the femoral cartilage are removed. In this work, researchers discuss the similarities and distinctions between the two distinct forms of knee cartilage. Authors suggest more approximation techniques, such as online SVMs, after relaxing the halting condition in the quadratic programme solver used for batch SVM training. This was done in order to provide room for alternative approximation methods. The two-stage procedure reached a higher level of accuracy when contrasted with the method now considered to be state-of-the-art in the field. It demonstrated greater inter-scan segmentation repeatability compared to the state-of-the-art technique currently in use, as well as a radiologist.

In their research on knee cartilage segmentation utilizing deep learning for characteristics, Prasoon *et al*. [72] at the following conclusions: Convolutional neural cell networks with three layers of complexity. For the purpose of image classification, deep learning systems like CNNs and other convolutional neural networks may be able to infer a hierarchical representation of the images they process. A team of authors devised an innovative method for classifying voxels in their work. It is possible to establish one-to-one links between the three 2D CNNs and the three 3D planes that make up a 3D picture. These three planes are denoted by the notations xx, yx, and zx, respectively. The authors created a method for segmenting low-field knee MRI pictures and used it on 114 scans that had never been published before. In contrast to the current technology, which utilizes 3D characteristics on numerous scales, the method developed by the authors uses just 2D features at a single scale in its analysis, making it more effective. Second, the characteristics and the classifier have been revised to align with the aim now being pushed forward.

Longitudinal Three-Label Segmentation of Knee Cartilage was a study carried out by Shan *et al*. [73]. The gradual cartilage degeneration in osteoarthritis patients calls for accurate segmentation methods independent of human involvement (OA). The author provides several unique approaches to three-label segmentation in order to improve the consistency of segmentation over time in longitudinal image data.

In order to handle the problem of cartilage segmentation in an improved way, use a segmentation approach that uses three labels, simulation of the longitudinal three-label segmentation technique is accomplished by using a convex optimization problem. The authors had previously implemented a segmentation system with three labels, but we have now added temporal consistency to it as well. It is possible that the segmentation may be recast as a convex problem, which would then provide the best solution. It is possible to compute anything along these lines. In order to do longitudinal segmentation, a pipeline that can autonomously segment knee cartilage is used. According to the results of the studies, adopting longitudinal segmentation rather than temporally independent segmentation results in more consistency in the segmentation process. This assertion requires a reference in order to be considered valid.

Gan *et al*. [76] presented the Multilabel Graph-based Approach for Knee Cartilage Segmentation. Data from the Osteoarthritis Initiative were used to conduct this analysis. Knee osteoarthritis is one of the most debilitating illnesses a person may suffer from.

Random walks may be used to effectively segment a huge number of objects, and it also has the potential to lead to the discovery of the global shortest route solution. It's possible that the pathophysiology of osteoarthritis may be better understood with some quantitative research. Random walks were more effective at knee cartilage segmentation than hand segmentation when compared to it.

In the process of extracting objects from an MRI scan, Kubicek *et al*. [75] used a newly invented fuzzy-based approach. To identify certain characteristics, the MRI data used in this investigation are segmented using a number of different approaches (MRI). Imaging of the knee is used to perform procedures such as the extraction and identification of the articular structures of the knee. Because even the smallest change in brightness might signal injury to the cartilage in joints, this subject is of significant interest to medical professionals. Creating colour maps of tissue densities *via* image segmentation is possible. This method uses a membership function based on detecting local extremes in the histogram to assign picture density to an output set. Each of these sets may be categorized according to a number of different colour swatches and palettes. It is possible to differentiate between different tissue forms based on density.

Gan *et al*. [76] presented their work on a binary seeds auto-generation model in order to achieve their objective of segmenting knee cartilage. In medical image analysis, picture segmentation is an essential step that may be performed. In addition, the manual, semiautomatic, and automated techniques of segmentation have all been shown to be useless in the ongoing study that has been carried out. To perform properly, models and processes need to use human input and data for training. It has been shown that computer-aided learning algorithms, along with other types of learning algorithms, are unsuccessful when it comes to identifying anatomical differences. An algorithm has been shown to be capable, *via* deep learning, of independently producing binary seed sets without requiring the participation of a human operator in the process. In order to compare the reproducibility of the proposed model to that of manual segmentation, normal and osteoarthritic magnetic resonance imaging of the knees was employed in conjunction with an algorithm for analysis. This came to light while comparing the proposed model's findings with those of manual segmentation. According to the author's evaluation, using the model for deep learning segmentation may be fruitful.

The knee joint is one of the elements of the human motion system that is often damaged. Because it provides direct and noninvasive pictures of the whole knee joint as well as the cartilage tissue, magnetic resonance imaging (MRI) is the most effective imaging modality for detecting structural changes in cartilage tissue. This is because MRI can detect structural changes in cartilage tissue. Revathi *et al*. [77] proposed a cartilage segmentation of knee osteoarthritis derived from magnetic resonance images (MRI). In this study, magnetic resonance (MR) imaging of a knee illustrates one approach to separating the cartilage in the knee. The author develops two different segmentation processes, one after the other, to arrive at the morphological operations of the final segmentation process. In terms of the quality level, this research's findings imply that the methodology can properly segment cartilage areas. The results of the newly developed methodology and those of manually segmented cartilage were compared and contrasted with one another. Due to the fact that it is a non-invasive method of measuring cartilage composition, the T2 relaxation time obtained using magnetic resonance imaging (MRI) has the potential to serve as an early biomarker for osteoarthritis of the knee.

The research conducted by Viken *et al*. [78] used a deep neural network to detect photographs taken during actual arthroscopy procedures to automatically separate the cartilage of the joints from one another. It was found that machine learning approaches might be used to handle the challenging task of categorizing and segmenting medical photographs since they are successful. This was discovered after it was determined that these techniques were effective. The fact that these strategies have been shown to be effective was the primary consideration that led to the formation of this judgement. In the area of medical imaging segmentation, multifractal analysis has also found significant use in recent years. To carry out automated segmentation, this study recommends using neural networks in conjunction with multifractals as a tool. In order to provide evidence in support of the thesis, a real arthroscopy photograph that was obtained while the patient was under anesthesia was used. It has been shown that the design of MultiResUnet is a great fit for carrying out pixel-perfect segmentation. It has been shown that the neural network classification of multifractal characteristics works well compared to other kinds of research.

Kessler *et al*. [80] used CNN to partition the data they collected from knee MRIs. Following the completion of the segmentation, a three-dimensional analysis of the morphology and content of the cartilage was carried out. In order to train U-Nets for the segmentation of femoral bone, tibial bone, and cartilage, data from the Osteoarthritis Initiative (OI) was used (OAI). DESS photos were used to generate U-Nets, which were then utilized to automatically segment bone-cartilage structures (the segmentations of bone and cartilage integrated into one structure) from the images.

An investigation of the morphology (thickness) and composition (T2) of cartilage was carried out with the assistance of surface-based 3D cartilage surface mapping (3D-CaSM), which included both manually performed and network-generated segmentations from OAI ZIB testing pictures. This was done by combining the bone and cartilage segmentations into one structure. After collecting cartilage thickness and T2 data from both U-Nets, the information was subjected to Bland-Altman tests to see how well it compared to manual segmentations. The findings were correct to a significant degree. The findings demonstrated that the data obtained were correct to a significant degree. For femoral and tibial cartilage thickness measurements, Bland-Altman analysis revealed a

mean bias [95 percent limits of agreement] of -0.12 to 0.33 [-0.28, 0.96] mm with 2D U-Net and 0.07 to 0.14 [-0.14, 0.39] mm with 3D U-Net. The mean bias [95 percent limits of agreement] for T2 ranged from -0.16 to 1.32 [-4.71, 4.83] ms for 2D U-Net and from -0.05 to 0.46 [-2.47, 3.39] ms for 3D U-Net. The 95 percent confidence intervals varied from -0.05 to 0.46 [-2.47 to 3.39] ms, while the mean bias for 2D and 3D U-Net was anywhere from -0.16 to 1.32 ms [-4.71 to 4.83] ms for T2.

Most knee cartilage segmentation techniques have been defined, and they may be used for volume measurements in DESS or SPGR sequences. In order to get T2 quantifications, these segmentations will first need to be put on T2 maps. Due to the time and manual alignment necessary for these operations, employing these techniques to analyze T2 maps in large clinical trials such as the Osteoarthritis Initiative (OAI) is challenging. Stehling *et al*. [82] devised a method for segmenting the knee cartilage for T2 values on MR imaging using data from the Osteoarthritis Initiative. The segmentation of one knee using DST and the measurement of T2 took an average of 63 minutes and three seconds (*vs*. 302 13 min for volume and T2 measurements with SST). Bland Altman plots revealed significant agreement between the two different segmentation techniques and the two readers when all three were compared. For the total knee cartilage mean T2, laminar analysis (up to 2.53 percent *vs*. 3.19 percent), and texture analysis, the errors in repeatability were the same for both DST and SST ($P > 0.05$). (up to 8.34 percent *vs*. 9.45 percent). The inter-reader repeatability errors in DST were much higher in the texture analysis (up to 15.59 percent) compared to the mean T2 and laminar analyses (up to 2.17 percent). Due to these discoveries, DST may be used in significant clinical investigations such as the OAI. In addition to being a cost-effective diagnostic tool, ultrasonic imaging (US) is non-invasive, does not use ionizing radiation, and is simple to transport.

The progression of knee osteoarthritis (OA) will lead to deterioration of the cartilage found in the knee. It is possible that changes in the shape of the knee joint cartilage may be seen in images processed in the United States using medical imaging technology. This study intends to propose a fresh technique to contrast enhancement that has the potential to overcome the limitations of the current method.

The gold standard method in research for grading osteoarthritis (OA) from thin tissue sections is histopathological grading, which has numerous known drawbacks. T. Frondelius *et al*. [83] previously developed a semi-automatic 3D grading system for human osteochondral plugs using micro-computed tomography (mCT) and phosphotungstic acid (PTA) as a contrast agent to capture complex three-dimensional (3D) OA-induced changes. T. Frondelius *et al*. ultimate goal is to automate the grading process, which requires accurate segmentation of different cartilage layers. The loss of attenuation contrast at the bone-cartilage (BC) interface, an important anatomical landmark, is a disadvantage of PTA staining. The author created a fully automatic BC interface segmentation method based on Deep Convolutional Neural Networks (DCNN) to address this issue.

Wirth *et al*. [84] investigated the T2 sub-regional MR spin-spin relaxation periods in osteoarthritic knees with and without loss of medial tibial cartilage for the purpose of the research that was published by the Osteoarthritis Initiative (OAI). The purpose of this study was to determine whether or not variations in the sub-regional laminar femorotibial cartilage spin-spin relaxation time (T2) over the course of one year are associated with eventual radiographic progression and cartilage loss in knees with established radiographic OA (ROA). As part of this case-control research, knees with medial femorotibial progression (OAI) were chosen for analysis based on a one-year decline in both quantitative cartilage thickness and femur length. This was done so that the knees could be compared with knees that did not have this condition. Radiography and magnetic resonance imaging are two modalities assessing the breadth of joint spaces (JSW). Both the male and female individuals had the same Kellgren-Lawrence grade (2/3), body mass index (BMI), and degree of discomfort. Using multi-echo spin-echo MRI, the T2 of the superficial and deep cartilage in sixteen separate femorotibial subregions was examined at the research's beginning and after one year had elapsed.

Si *et al*. [85] deliberated that it was extremely necessary for the research on osteoarthritis to evaluate cartilage thinning in a full knee joint and track changes in cartilage morphology over time in the general population. This was before massive volumes of imaging data and artificial intelligence were integrated. As a part of the research, the authors will be analyzing the thickness of the cartilage in the knee in a number of different anatomical areas. Furthermore, we will be determining whether or not there is a connection between age and the pattern of cartilage thinning in order to better understand this phenomenon. The participants in the research ranged in age from 15 to 64 years old, with the average participant being 35±10 years old. A total of 2,481 knees in good health were recruited for the study. The cartilage of the knees was segmented automatically and accurately using deep learning, and a computer algorithm was used to quantify the thickness of the cartilage in 14 distinct anatomical locations. In order to get a picture of the knees, a superconducting magnetic resonance imaging device operating at 3 T was used. When analyzing the thickness measurements using ANOVA, many variables were considered, including age, gender, and which side the measurements were collected from.

Using three-dimensional magnetic resonance (MR) imaging of the knee, Rania Almajalid *et al*. [86] observed the movement of knee cartilage over the course of one year as part of their research. The period of the trial was determined to be twelve months. The medial tibia compartment of the knee joint was the major focus of this examination. Both manual cartilage segmentation on each slice of the 3D MR sequence and the cartilage damage index (CDI) was used to quantify the thickness of the cartilage in this compartment. The CDI was used to do cartilage thickness estimates at a few distinct strategically critical sites. They used artificial neural networks (ANNs) to precisely show the varying pattern of cartilage thickness. The information on cartilage thickness and its immediate surroundings was a component of the data used to produce the input feature space. The input feature space was generated utilizing the data from the baseline year. According

to the difference in thickness that was assessed between the baseline year and the follow-up data that was gathered after a period of 12 months, the result categories were "changed" and "no change." The utilization of CDI data and manually segmented features were used in training a broad variety of artificial neural network (ANN) models.

Egor Panfilov *et al*. [87] Observed morphological changes in the knee cartilage sub-regions as one way to track the course of osteoarthritis. These changes are most often recognized *via* magnetic resonance imaging (MRI). Till now, cartilage segmentation has been carried out manually, with a significant amount of attention to detail. Although deep learning methods make it feasible to automate the process, the assessment these algorithms provide is not clinically acceptable. As part of their review of the link between the radiographic progression of osteoarthritis and segmentation and sub-regional assessment of articular cartilage, the authors present and evaluate a completely automated approach. This was done as part of their research into the relationship. This is done as part of their review of the link between these two aspects, and it is an important component of the investigation. The findings obtained from the Osteoarthritis Initiative (OAI) using 3D double-echo steady-state MRI were presented in two distinct sets. In the first set, the sample size was n = 88, while in the second set, the sample size was n = 600. The data in each set came from visits at 0, 12, and 24 months after the first one. The sub-regional volume and thickness of the knee cartilage tissues were obtained by applying deep learning-based segmentation in conjunction with multi-atlas registration. The initial batch of data that was obtained was used to create and test the segmentation model. This was done utilizing the data. When analyzing the second batch of data, the authors compared and contrasted the morphological measures obtained using the method with the one used before. In addition, in a retrospective study, their ability to distinguish between the progression of radiographic osteoarthritis over the period of 12 and 24 months was assessed.

Deep neural networks may be used in order to segment the cartilage found in the knee Ichiro Sekiya *et al*. [88]. With a total of 45 sub-regions and 9 regions, this programme was used to analyze the interscan measurement error in terms of cartilage thickness and expected cartilage area ratio. Following this, each of these sub-regions was divided further, this time into regions. For the objective of this study, magnetic resonance imaging (MRI) scans were carried out on the brains of ten healthy volunteers twice throughout the span of a single day. The total cartilage thickness of 9 areas and 45 sub-regions were calculated by the algorithm, and no changes from humans were necessary at any point in the process. In addition to this, the anticipated cartilage area ratio was established (thickness 1.5 mm).

The interscan measurement error was evaluated for each area and sub-region by utilizing data from nine distinct donors, except for one donor who had MRI motion while the scanning was done. This donor was excluded from the evaluation. All nine areas and 39 of the 45 subregions were scanned for cartilage thickness, and the error in the interscan measurement was less than 0.10 millimeters across the board.

Knee magnetic resonance imaging (MRI) is one of the best imaging modalities to determine the severity of OA. It has been shown to be predictive of outcomes after surgeries such as arthroscopic partial meniscectomy. However, manual grading of cartilage disease using semi-quantitative grading systems is time-consuming and suffers from inter-observer variability limiting its routine use in clinical practice. Many researchers have developed manual, semi-automatic and fully-automatic methods to accurately segment the cartilage. Deep Learning based methods outperform all the existing state-of-art methods.

2.3. Meniscus Segmentation & Quantification of Damages

The meniscus is very important to the function of a healthy knee joint because of its ability to absorb stress and evenly distribute the load. MRIs of the knees of people with osteoarthritis (OA) often demonstrate meniscal damage. Rip patterns that are horizontal, flap-like, or more sophisticated may be indicators of meniscal maceration or full destruction. MRI scans of the knees of middle-aged and older individuals often reveal asymptomatic meniscal abnormalities in the knees of these patients. Studies have demonstrated that meniscal abnormalities are associated with the development of radiographic osteoarthritis [89], the development of cartilage loss [90], and the progression of cartilage loss [91]. Meniscal abnormalities have also been linked to the loss of cartilage. It is necessary to segment the menisci into three dimensions in order to calculate quantitative meniscal measures such as meniscal volume and tibial coverage. The primary emphasis of many current lines of investigation in the field of meniscus research is the development of computer tools for segmenting and measuring changes in the meniscus. Table **3** provides an example of a method introduced after 2010, including full automation.

Table 3. Automatic segmentation of meniscus: Existing studies (After the year 2010).

Study/Refs.	MR Pulse Sequence	Technique Used	Sensitivity (%)	Specificity (%)	DSC
Zhang *et al*. 2013 [40]	Multi-contrast	DRF + ELM	0.8395	0.9934	0.82
Felicia *et al*.2017 [45]	3D T1 WE T2 de3D WE	2DUNetcascade- deep learning	0.784	1.000	DSC- 0.75 3
Norman *et al*. 2018 [46]	T1 weighted images and three-dimensional (3D) double-echo steady-state (DESS) images	U-Net convolutional network	-	-	Mean validation Dice coefficients 0.833 (95% CI: 0.821, 0.845) for meniscus.

(Table 3) contd.....

Study/Refs.	MR Pulse Sequence	Technique Used	Sensitivity (%)	Specificity (%)	DSC
Paproki *et al*. 2014 [92]	Double-echo steady-state MR images	Deformable model approach.	MD: 78.9 95% CI: 77.4-79.9	MD: 99.99 95% CI: 99.99 -99.99	-
	3D weDESS	3D ASM	MM-0.771 ML- 0.790	MM- 0.999 ML- 0.999	MM- 0.783 ML- 0.839
Tack *et al*. 2018 [93]	2D DESS MRI slices	CNNs in combination with Statistical Shape Models (SSMs)	-	-	Dice Similarity Coefficient: MM - 83.8%, LM -88.9%
Bloecker *et al*. 2012 [94]	Sagittal double-echo steady state with water excitation magnetic resonance sequence	Characterize tibial plateau coverage and morphometric differences of the medial (MM) and lateral meniscus (LM) in a male reference cohort using three-dimensional imaging	-	-	-
Zarandi *et al*. 2016 [95]	3D knee T1-weighted and T2-weighted MR images	A type-2 fuzzy expert system for meniscal tear diagnosis using PD magnetic resonance images (MRI)	91.84%	-	-
Zhang *et al*. 2019 [96]	3-T clinical MR scanner	A detailed finite element model of the knee joint with bones, cartilages, menisci and main ligaments	-	-	-
Couteaux *et al*. 2019 [97]	Sagittal MR images centered around the knee	Mask region-based convolutional neural network (R-CNN)	-	-	Score of 0.906
Michal Byra *et al*. 2020 [98]	3D ultrashort echo time (UTE) cones MR imaging	2D attention U-Net convolutional neural networks for the menisci segmentation	-	-	An automated method with dice scores of 0.860 and 0.833. Manual segmentation achieved 0.820
Benjamin Fritz *et al*. 2020 [99]	One hundred consecutive patients' MR Images.	Fully automated deep convolutional neural network (DCNN)	-	-	For medial meniscus tear detection, sensitivity, specificity, and accuracy were for reader 1: 93%, 91%, and 92%, for reader 2: 96%, 86%, and 92%, and for the DCNN: 84%, 88%, and 86%. For lateral meniscus tear detection, sensitivity, specificity, and accuracy were for reader 1: 71%, 95%, and 89%, for reader 2: 67%, 99%, and 91%, and for the DCNN: 58%, 92%, and 84%
Zhongjie Long *et al*. 2021 [100]	T2-weighted MR slices/frames	ATTU-Net	-	-	Min DSC 0.743 Max DSC 0.990 Average DSC 0.864 ± 0.077
Yuan-Zhe Li *et al*. 2022 [101]	Philips 3.0 T MRI system	3D deep convolutional neural network (DCNN)	90% sensitive	-	DCNN model, AUC value, accuracy, sensitivity, and specificity values in the test set were 0.907, 0.924, 0.941, and 0.785, respectively
Swanson *et al*. 2010 [138]	T2 Map 120 mm field of view MRI obtained from 3 T Siemens machines	Semi-automated segmentation consisted of five phases: initialization, threshold determination, segmentation, conditional dilation, and morphological post-processing	-	-	-

I. Pang *et al*. [43] presented their research, Automatic Articular Cartilage Segmentation Based on Pattern Recognition from Knee MRI Images. In order to better understand how cartilage is segmented in MRI scans of the knee, an automated approach is used. The femoral cartilage, the tibial cartilage, and the patellar cartilage are all segmented using the Bayesian theory in conjunction with three binary classifiers based on the integral and partial pixel qualities. The first steps entail devising an iterative approach for selecting an acceptable threshold for the Canny operator and extracting the bone-cartilage interface from MRI images. These steps are part of the first attempts. As a second example, the one-of-a-kind edges are recognized by particular characteristics, making it possible to separate the various cartilage types simultaneously. The cartilage edge and the anatomical region it occupies contribute to accelerating the segmentation process. Morphological treatments have the potential to improve the outcomes of the final segmentation. The smooth cartilage border presented by the automated segmentation is consistent with that seen in the human segmentation.

Random Forest and the deep learning method of 2D UNet fully convolutional networks (FCN) were used by the research team led by F. Aldrin *et al*. [45] to differentiate among menisci. For the purpose of extracting menisci from 3D MRI images, both approaches were evaluated and compared in a series of tests. In contrast to Random Forest, a 2D UNet cascade achieved a Dice Similarity Coefficient (DSC) of 75.3%, while Random Forest only achieved 54.43%.

Researchers looked at 28 more participants' distal femurs and articular cartilage using 3D MR images and the 2D UNet cascade. When applied to both the distal femur and the articular cartilage, the single-class 2D UNet cascade produced noticeably more favorable results.

In order to assess relaxation and morphology, B. Norman *et al*. [46] investigated the use of 2D U-Net Convolutional Neural Networks for automated cartilage and meniscus segmentation of knee MR imaging data. This was done in order to analyze the data. This study utilized quantitative magnetic resonance imaging (QMRI) to determine the accuracy and precision of automated segmentation of morphology and relaxometry in quantitative magnetic resonance imaging (QMRI) for degenerative knee disorders such as osteoarthritis. These disorders include knee degeneration (OA).

The models provided an independent segmentation in an average of five seconds. The human and automated quantifications of T1 and T2 values, respectively, had correlations that averaged 0.8233 and 0.8603 and 0.9349 and 0.9384, respectively. These correlations were found to be significant. The automated approach's long-term accuracy is comparable to that of the human method. These findings provide evidence of the accuracy and precision with which U-Net can create segmentations. These segmentations have the potential to be used in the diagnostic process of OA in order to get relaxation durations as well as morphological characteristics and values.

Semi-automated segmentation was proposed by M. Swanson *et al*. [102 - 138] in order to evaluate the lateral meniscus in knees that were either healthy or had osteoarthritis. The segmentation approach was used on ten normal controls and fourteen osteoarthritis patients who did not have symptoms or risk factors for developing knee osteoarthritis. These patients were part of the Osteoarthritis Initiative (OAI). A threshold level was formulated using a Gaussian fit model after hand-selecting a seed point in the meniscus. In order to fulfill the requirements imposed by the anatomy and the intensity, a threshold operation was carried out, and this was then followed by conditional dilation and post-processing. During the post-processing stage, an accuracy check is performed on the region around the meniscus by reevaluating the included and excluded pixels. Both normal and degenerative menisci were subjected to a head-to-head comparison between the results of the segmentation algorithm and those of the manual segmentation, which five human readers performed.

Using MRI data from the Osteoarthritis Initiative, A. Paproki *et al*. [92] suggested automatically segmenting and analyzing normal and osteoarthritic knee menisci. An automated approach for segmenting and measuring the medial and lateral meniscuses of the knee will be put through its paces using magnetic resonance (MR) images of the knee (MM and LM). The author conducted analyses of OAI cohort photographs utilizing sagittal water-stimulated double-echo steady-state MR images. These images were acquired in a sagittal plane. A deformable model technique was used in order to carry out an automated segmentation of the MM and LM inside the MR images. Data on tibial coverage and subluxation were automatically produced to facilitate the comparison of knees that displayed varied degrees of radiographic osteoarthritis and medial and lateral joint space narrowing (mJSN, lJSN) and discomfort (Wilcoxon tests).

The menisci of the knee may be segmented utilizing an innovative approach reported by A. Tack *et al*. [93] and can be seen in MR images. It is possible to evaluate osteoarthritis (OA) biomarkers using meniscal measurements. This work offers a unique approach for autonomously segmenting the knee's menisci using MRI images as the primary data source. Biomarkers of osteoarthritis may be quantified using meniscal measurements in certain cases (OA). Constructing a segmentation approach used convolutional neural networks with statistical shape models.

88 manual segmentations were used to determine how accurate the results were. We estimated the meniscal volume and tibial coverage, then looked for differences between the OA, JSN, and pain (WOMAC) groups. Six hundred individuals were investigated to see whether or not there was a connection between the results of MOAKS specialists and the computerized meniscal extrusion. In order to determine whether or whether biomarkers might accurately predict the presence of radiographic osteoarthritis in 552, a conditional logistic regression was carried out (184 with incident OA and 386 controls). The medial menisci were dichotomized and segmented in a very precise manner.

K. Bloecker *et al*. [94] investigated the medial and lateral menisci of healthy boys' knees using magnetic resonance imaging (MRI). Utilizing three-dimensional imaging, the objective was to determine what percentage of a reference group's medial and lateral menisci were covered by the tissue in question. For the purpose of this study, the researchers employed a sagittal double-echo, steady state, water excitation MRI sequence (slice thickness: 1.5mm, pixel resolution: 0.37 x 0.70mm), as well as multiplanar reconstructions, on a total of 47 men who were a part of the Osteoarthritis Initiative reference cohort. Complete knee coverage was attained by hand-segmenting the LT plateau cartilage and the MM and LM knee joint surfaces. This led to the achievement of the goal. A coronal intermediately weighted turbo spin echo was used to assist with this method. Estimates were made in three dimensions for the total menisci, the body of the menisci, the anterior and posterior horns of the menisci, and the tibial coverage.

Tears in the meniscus are one of the most common knee problems affecting young athletes as well as the elderly, and it is essential to make an appropriate diagnosis and undergo surgical intervention if necessary. Because it is difficult to manually diagnose meniscal tears and because of the possibility of mistakes being made, automatic detection

approaches are required. M. Zarandi *et al*. [95] developed a type-2 fuzzy expert system as a means of identifying meniscal tears via the use of PD magnetic resonance imaging. (MRI). The Type-2 fuzzy image processing paradigm comprises many components, the most notable of which are the pre-processing, segmentation, and classification stages. An enhancement algorithm is applied to the data to start the pre-processing. In order to complete the processing of the pictures, It2PCM may make use of the results that were produced by Interval Type-2 Fuzzy C-Means (IT2FCM). After that, IT2PCM will utilize those outputs to further process the photos. We have to go back and tweak the value in order to further improve IT2PCM. Two-layered perceptron networks are often used during the classification process. Compared to a method of meniscal tear identification that is more widely used, the segmentation technique, a type-2 expert system that has been suggested, provides more accurate results.

K. Zhang *et al*. [96] conducted a finite element study to investigate meniscectomy's effects and the meniscus's following degradation of the knee joint. In order to determine the effect that degenerative and radial meniscal tears, as well as meniscectomy, have on the knee's biomechanics, these conditions will be investigated. Using computed tomography and magnetic resonance imaging data, a model of the knee joint was created, which included all of the bones, cartilages, menisci, and ligaments that make up the joint. The model was subjected to simulated vertical and anterior stresses, which mimicked the model's static position and minimal bending. This was done in order to detect both the menisci's degeneration and the resulting medial meniscectomy. When compared to the effects of compression and shear stress, the extrusion of the meniscus was shown to be superior. This task has been finished. In degenerative and radial rips, there is a substantial association between medial meniscal tear stress and extrusion values, higher peak meniscal and cartilage compression and shear stress, and severe meniscus extrusion. Patients suffering from knee ailments may find that computer-assisted diagnosis and treatment planning benefit their condition thanks to the 3D segmentation of knee joint tissues.

Because of the difficulties and unpredictability associated with completing human segmentation across various raters, there is a clear and present demand for automated segmentation methods. In order to successfully separate human tissues, a variety of approaches have been used. For instance, it is still challenging to dissect the microscopic menisci that are located in the knee.

V. Couteaux *et al*. [97] provided evidence that the Mask-RCNN can detect and classify knee meniscus tears. Participants were asked to identify the existence of tears in the anterior and posterior menisci as well as the direction of these tears after having sagittal MRI slices cropped around the knee (horizontal or vertical). An R-CNN was trained to differentiate between normal and torn menisci. After that, it was reinforced using ensemble aggregation to enhance its robustness. Finally, it was cascaded into a shallow ConvNet in order to identify the direction of tearing in the meniscus. The database provided for the challenge contained correct predictions of tears based on the V. Couteaux technique. For all three tasks, this approach produced a weighted AUC score of 0.906, placing it first in the competition. For non-typical cases of severely injured menisci or many tears, expanding the database or using 3D data may help further improve the performance.

Yi Wang *et al*. [101] investigate the possibility of automatically recognizing a torn meniscus in the sagittal and coronal planes of the knee joint using radiomics fusion as their research method. Between July 2018 and March 2019, the institution's Department of Orthopedics admitted 152 patients with arthroscopically confirmed meniscal injuries. These patients were treated at the facility. Using sagittal and coronal pictures acquired in single mode, 1316 dimensional radiomic signals were obtained for the menisci.

In order to construct a dual-mode joint feature group with 2632-dimensional radiomic fingerprints, the characteristics from the sagittal and coronal planes were joined. For the most significant 8-dimensional radiomics signatures, the ICC values for Model 1 ranged anywhere from 0.832 to 0.998, while the ICC values for Model 2 ranged anywhere from 0.845 to 0.998. For both the training and validation sets, Model 3 had an AUC of 0.947, which was significantly higher than the other two models, which had AUCs of 0.889 and 0.876, respectively (AUCs of the training set and validation set were 0.831 and 0.851, respectively).

Lee *et al*. [102] developed a method for knee cartilage segmentation from magnetic resonance (MR) images. The process of segmentation included the construction of several atlases, the use of a locally weighted vote (LWV), and the reorganization of geographic regions. All of the training examples were first registered with the help of a target picture, and then the best-matched atlases were chosen. Researchers have used an LWV strategy to merge the data from the two atlases in order to get to the first segmentation result. This allowed us to more accurately represent the data. The first segmentation result produced bone, cartilage, and nearby regions data. This data was used. Producing seed points for the graph-cutting approach used statistical data as input. In the end, the outliers and aberrant bone sections were reevaluated as part of the region correction technique.

A comparison of the effects of loaded *vs*. unloaded knee MRI on meniscus extrusion was conducted by Rina Patel *et al*. [103] in research including healthy volunteers as well as patients suffering from osteoarthritis. The extrusion of the meniscus is the topic of this study, which examines both healthy persons and those with varying degrees of osteoarthritis (OA). Unloaded and loaded three-dimensional magnetic resonance imaging scans of the knees were performed on a total of 143 healthy participants and OA patients. The Kellgren-Lawrence (KL) approach was used in order to evaluate OA. It was found that there were tears in the meniscus. The mean and standard deviation were used to represent the descriptive data. A comparison between the groups that were loaded and those that were emptied was carried out with the use of the Student t-test. When the p-value was less than 0.05, it was determined that all of the computations were statistically significant. There were a total of 87 female participants and 56 male participants in the study, with an average age of 53 years old and a standard deviation of 9.7 years.

The following is the grade distribution, as determined by Kellgren-Lawrence: There were 46 cases of grade 1 meniscus tears, 25 cases of grade 2 meniscus tears, 13 cases of grade 3 meniscus tears, and three cases of grade 4 meniscus tears among the patients who had grades 0 and 1. Significant differences were seen in the medial meniscal extrusion when comparing loading and unloading conditions (p 0.0001). When the medial meniscus was loaded and unloaded, there were statistically significant differences in KL score groups 0, 1, and 3. It was determined that loading and unloading did not significantly impact the lateral meniscus extrusion (p = 0.07). After loading the device, patients with low KL values (between 0 and 1) and those with a KL score of 3 improved their medial meniscal extrusion. It is possible for a loaded MRI scan to provide a more accurate diagnosis of medial meniscal extrusion, particularly in patients with little to moderate osteoarthritis.

Treating complicated rips in meniscal ligaments was the topic of research conducted by Nobutake Ozeki *et al*. [104]. After suffering an injury, a meniscal repair should be the first course of therapy chosen so that the meniscus may remain healthy and functional. Meniscal repair, on the other hand, has been shown in long-term follow-up studies to have superior clinical results and less severe degenerative changes in osteoarthritis. In addition to bone marrow stimulation and platelet-rich plasma injections, fibrin glue, stem cell injections, and scaffolding have all contributed to the expansion of the applications of meniscus surgery. Individuals with damage to their meniscus that were formerly thought to be irreversible now have a viable option for meniscus repair due to advancements in the treatments used to heal the injury and biological augmentation.

2.4. Different Methods for Knee Joint Segmentations based on MRI

2.4.1. Active Contour for Knee Joint Segmentation

One of the active models in image segmentation techniques is the active contour. It separates the region of interest by utilizing energy constraints and forces in the image. Active contours are used to segment regions from medical images such as brain CT and MRI scans. Many researchers have used the active contour method for knee joint segmentations, as illustrated in Table **4**.

2.4.2. The ASMs and the AAMs for Knee MRI Segmentation

Active Shape Model (ASM) and Active Appearance Model (AAM) segmentation techniques are widely used in the field of medical imaging due to their accuracy. This segmentation technique has been used by many researchers to accurately segment bone and cartilage from MR images. Table **5** explains how to segment different knee joints using AAM and ASM.

Table 4. Active Contour for Knee Joint Segmentation.

Method	Publication	Target	Weakness
Geodesic Active Contour.	Lorigo *et al*. [105].	Bone	The GAC snake model was sensitive to edge clarity.
Cubic B-spline; Bezier Spline.	Cohen *et al*. [106], Lynch *et al*. [107], Carballido-Gamio *et al*. [108, 109].	Cartilage	A further process was needed for these methods; The methods were sensitive to initialization; The optimization was non-convex; The convergence was not guaranteed.
Directional GVF Snake.	Tang *et al*. [110].	Cartilage	The GVF snake model could not handle long, thin, concave shape.

Table 5. ASMs and the AAMs for Knee MRI Segmentation.

Authors	Model	Targets	Weakness
Solloway *et al*. [111]	ASM (2D)	Bone/Cartilage	1. 3D structures were ignored in the model. 2. Post-processing was needed.
Fripp *et al*. [57, 92, 104], Schmid *et al*. [118, 119].	ASM (3D)	Bone	1. The search for an initial model pose parameters can be very time-consuming. 2. The initialization was based on manually defined landmarks.
Gilles *et al*. [112], Seim *et al*. [17].	ASM (3D)	Bone/Cartilage	1. Such models only reach a local optimum and depend heavily on their initial position; 2. The cartilage segmentation largely depends on the preset parameter ‘thickness.'
Vincent *et al*. [113], Williams *et al*. [114, 115].	AAM	Bone/Cartilage	Variation outside these spaces cannot be properly captured if no subsequent relaxation step is used;

Table 6. VC-based Methods for Knee Joint Segmentation.

Authors	Classifier	Pros	Cons
Dam *et al.* [12]	KNN	The rigid multi-atlas registration allowed the multi-structure segmentation.	4. A large number of training samples are needed.
Folkesson *et al*. [36]	KNN	The method could segment knee MRI fully automated.	---
Shan *et al*. [39]	Probabilistic KNN	The spatial prior generated by multi-atlas registration improved both performance and computational efficiency.	1. Very low computational efficiency;
Prasoon *et al*. [71]	CNN	The introduced deep feature improved	-
Prasoon *et al*. [72]	KNN+SVM	The computational efficiency was improved by using two-stage classification framework.	-
Folkesson *et al*. [139, 140]	KNN	The combination of two-class KNN outperformed the three-class KNN [71].	-
Wang *et al*. [116]	KNN	The introduced novel multiresolution patch-based segmentation framework allowed a coarse-to-fine segmentation.	2. Over-segmentation on the BCI;
Liu *et al*. [117]	Random Forest	Improved the performance by introducing context information.	3. The training process is time-consuming;

Table 7. Comparisons of Different Methods.

Method	Pros.	Cons.
SSMs and AAMs	1. The methods could be fully-automatic. 2. The models could handle incomplete boundaries well.	1. The methods have difficulties for cartilage modeling. 2. The performance largely depends on the representativeness of the training samples.
Active Contour	1. Low computational complexity. 2. The methods could achieve accurate results with expert interaction.	1. It is hard to build an automatic system based on active contour. 2. Convergence problem.
Voxel Classification	1. Concise model. 2. High accuracy. 3. The performance could be improved by providing more training samples.	1. Over-segmentation and the need of post-processing. 2. Computational complexity is high.
Graph-based	1. High accuracy. 2. Global optimization could be achieved.	1. High computational complexity and high storage requirement; 2. Initialization is needed in most cases.
Atlas-based	1. High accuracy. 2. The process and the results are intuitionistic.	1. Existing labeled slices should be provided; 2. Difficulties in handling the variations

2.4.3. VC-based Methods for Knee Joint Segmentation

Different VC-based methods are applied in order to segment knee joints from MR Images. Table **6** are those that focus on the development of computational algorithms for segmenting knee joints from knee MR data.

2.5. Comparisons of Different Methods

Table **7** shows the comparison of different methods of segmentation with their advantages and disadvantages.

By employing simplex meshes, B. Gilles *et al*. [112] presented a novel method for segmenting and registering images of the musculoskeletal system. Previous studies have demonstrated that discrete models may be helpful when it comes to the segmentation of medical images. The framework's inventor has included multi-resolution approaches and a reversible medial representation to calculate geometry and non-penetration requirements more straightforwardly. The presented model enables registration between and within patients (involving rigid and elastic matching). Because of these representations, morphological analysis may be done more straightforwardly. The author uses a case study of the hip and thigh to illustrate that the muscles, bones, ligaments, and cartilages of the hip and thigh may be recorded quickly (30 minutes), accurately (1.5 mm), and with minimum manual labour. This is demonstrated via the usage of the hip and thigh.

In the study, Graham Vincent *et al*. [113] segmented MR images of the knee using a model-based technique. Active Appearance Models (AAM), constructed from manually segmented instances found in the Osteoarthritis Initiative database, are used in the segmentation method as the primary tool. An MDL Groupwise Image Registration approach is used

in order to construct model correspondences of a superior grade. Methods like multi-start and hierarchical modelling are used to fit the model to newly taken photographs. The model successfully segmented the test data from the MICCAI 2010 Grand Challenge, and it did so with a high degree of accuracy while making no modifications to the training data.

The solution presented is the automated segmentation of tibial articular cartilage from knee MRI data. Z. Wang *et al*. [116] reported on an application to knee MRI in their work titled "Patch-Based Segmentation without Registration."

This work presents a brand-new method for multi-resolution patch-based segmentation, and it does not need image registration to function properly. In addition, an image similarity measure based on directed gradients and a 3D histogram is also provided for use in atlas selection. This tactic was tested during the MICCAI SKI10 Grand Challenge, which included 100 different training atlases and 50 test photos that had never been seen before. Our approach did very well compared to the most cutting-edge techniques of knee MRI segmentation used in this competition; consequently, we received excellent evaluations and could imitate the best outcomes.

In order to differentiate between the bones and cartilages of the knee, it is required to segment MR images of the joint; in the article, Q. Liu *et al*. [117] explore the use of multi-atlas context forests to segment cartilages and bones sequentially. This technique uses training atlas pictures to repeatedly train sets of random forests to classify individual voxels to segment bone and cartilage. The preliminary segmentation results are used to produce context characteristics for the random forests that are a part of the iterative architecture. In order to derive characteristics pertaining to the context, the preliminary segmentation result of the topic has to be registered with a large number of atlases.

After that, the author uses the registered atlases to get the spatial priors of the anatomical labels. After that, we put those spatial priors to use in order to acquire more context about the topic. However, keep in mind that the early findings of the topic's segmentation, which have been revised, may cause these characteristics to shift. The accuracy of many atlases' registration to the subject also increases due to improved segmentation findings, which makes it possible to train random forests iteratively. The suggested technique has been put through its paces using the SKI10 dataset, and the results indicate that it is quite accurate.

In the setting of a restricted field of view, Schmid *et al*. [118, 119] presented statistical models for bone segmentation. The author of this paper presents a modified initialization for modelling and computer-aided diagnosis, as well as a multi-resolution SSM approach for the segmentation of MRI bone images produced in constrained FO*vs*. Both of these are presented in conjunction with a multi-resolution SSM approach for segmenting MRI bone images. Creating a dependable SSM in this research, which is based on both complete and corrupted forms and the simultaneous optimization of transformations and shape parameters, is an example of innovative research. 86 magnetic resonance imaging (MRI) scans of the femur and hip bones were used to construct an algorithm. Both the pixel density and the field of view of these photos have been significantly altered from one another. The segmentation findings may be used in an image-based clinical diagnosis if one so chooses (*e.g.*, an average distance error of 1.12 0.46 mm). Segmentation from medical pictures is especially difficult due to the structural complexity of the musculoskeletal system, as well as the great diversity of persons in the community and their potential for severe deformations.

In order to manage the biological diversity present in many medical imaging classification and segmentation tasks, a substantial quantity of training data is required. Training data points may have a significant impact on how well someone learns. There is a possibility that non-linear support vector machines (SVMs) with excellent generalization performance will not be considered (SVMs). In many medical imaging circumstances, the segmented object has a disproportionately small number of pixels or voxels compared to the backdrop. This results in an abnormally unbalanced population. A. Prasoon *et al*. [120] provide a two-stage classifier to solve the difficulties associated with large-scale medical imaging. Getting started using a classifier that can be easily trained utilizing extensive datasets is essential. This is done to ensure that the class imbalance may be exploited by modifying the classifier to detect the background in an acceptable manner. Only information that isn't background is carried over to the next level of processing. A strong classifier with a high training time complexity may determine whether individual data points belong to a certain entity.

The absence of spatial correspondence among individuals and time and the geographic heterogeneity of cartilage advancement across subjects make some analytical methods, such as subregion-based analysis, which have been developed to improve quantitative cartilage analyses, less than ideal. This is one of the reasons why it is difficult to apply analytical approaches. Detection of Diseased Regions in a Patient's Knee Using Longitudinal Magnetic Resonance Imaging Data by C. Huang *et al*. [121] concentrated on these two concerns in order to establish a statistical approach for measuring longitudinal cartilage in OA patients. The goal was to develop this method as quickly as possible. The first thing that must be done to analyze the data from 3D knee imaging is to search for patterns, both temporally and geographically. Gaussian hidden Markov models (GHMM) are used to explore the variance in cartilage progression over time and between individuals with OA.

In the suggested technique, a pseudo-likelihood function and an expectation-maximization (EM) approach are used to estimate the unknown parameters of the GHMM that are the most accurate possible. Using the recommended approach, it is possible to accurately detect each OA patient's unhealthy locations, and the longitudinal cartilage thickness of each latent subpopulation may be evaluated in great detail.

Through the Osteoarthritis Initiative (OAI), researchers can acquire clinical records, images, and biospecimens open to the public. These resources can be used in the study of factors that contribute to the onset and progression of OA, as well as the evaluation of biomarkers that can predict and monitor the

progression of the disease. In their Perspectives, F. Eckstein *et al*. [122] address imaging processes and outline image analyses that have been done so far for the OAI cohort and its design. Additionally, they describe how the OAI cohort was designed. The longitudinal changes in cartilage thickness that occurred within the OAI progression subcohort over the course of two years are accounted for in the author's descriptive analysis of these data from a core sample consisting of 600 knees taken from 590 individuals. These researchers also highlight how the methodological and applied imaging data obtained from the OAI pilot study may be used to generate biomarkers to assess the success of intervention studies. They provide greater elaboration on this point.

Computer-aided knee MRI segmentation has immense potential in clinical diagnosis, as well as in scientific research. The central issue in knee MRI segmentation is finding the bone and cartilage boundary accurately. For bone segmentation, the existing literature supports that the deformable model-based methods can handle bone segmentation well. The region-growing-based semi-automatic methods also achieve satisfactory results. Voxel/pixel classification-based methods could handle bone segmentation well. However, researchers prefer deformable models for bone segmentation due to the higher computational efficiency. The segmentation of articular cartilage still needs further investigation, especially the fully-automatic cartilage segmentation.

Using quantitative computed tomography of the knee, P. Zerfass *et al*. [123] developed a unique integrated approach for assessing bone mineral density (BMD) and subchondral bone structure. The establishment of anatomical coordinate systems is followed by the acquisition and reconstruction of pictures in three dimensions, followed by the positioning of analysis volumes of interest (VOI) in a consistent manner. Researchers have developed new segmentation algorithms that can reliably identify the growth plates of the tibia, femur, and joint space. There are five separate VOIs on the epiphysis, and each one is located at a different distance from the articular surface. Further differentiation is made between the medial and lateral components of each VOI. BMD is determined for each VOI that is examined. Quantifying the subchondral bone structure may be accomplished by doing a texture analysis on a high-resolution CT reconstruction created using a CT scan. For every VOI that was investigated, local and global homogeneity and anisotropy were subjected to measurement. The overall accuracy of the method over a shorter period of time was evaluated by taking duplicate measurements of twenty human cadaver knees that had osteoarthritis.

R. Youssef *et al*. [124] used semi-automatic compartment extraction to measure the 3D bone mineral density and the morphometric properties of the subchondral bone. This was accomplished by using CT scans. The study aims to develop a semi-automatic method of segmentation of the subchondral bone in the tibial compartments of the knee to assess 3D local variation of BMD and BV/TV from HR-pQCT images. Because of osteoarthritis of the knee, the author discusses a unique semi-automatic method for assessing bone mineral density (BMD) and bone ratio (BV/TV) in clinically important compartments (medial *vs*. lateral) (anterior versus posterior). This convex-hull method was developed mainly for high-resolution peripheral computed tomography, but it has the potential to be employed in clinical CT if the resolution is high enough.

An innovative method for knee cartilage segmentation that combines deep segmentation networks with bone-cartilage complex modelling has been created, as stated by Hansang Lee *et al*. [125]. The diagnosis and treatment of osteoarthritis are both significantly aided by the segmentation of cartilage on MRIs of the knee. Recent research has demonstrated that deep segmentation networks, also known as DSNs, may be helpful in the process of segmenting cartilage. DSNs tend to gloss over minute details like cartilage when they are learning multi-class segmentation, which is why they have limits when it comes to segmenting cartilage. This work used BCC modelling and BCD extraction to develop an innovative DSN-based cartilage segmentation approach. Because the DSNs have such a limited understanding of cartilage, the researchers H. Lee and colleagues suggest building a mask called the BCC, composed of bone and cartilage. In order to remove the cartilage, the bones holding them in place must first be removed. Once this step is complete, the cartilage may be removed. In addition, a 2.5-dimensional segmentation method is used. This method combines the outcomes of many segmentation masks applied to various planes using a majority vote to improve the accuracy of the segmentation even further.

In the dataset used to validate the SKI10 public challenge, our BCD-Net obtained average DSCs of 98.1 percent for the femoral cartilage and 83.8 percent for the tibial cartilage, respectively.

It is necessary to perform automated articular cartilage segmentation in order to conduct quantitative cartilage analysis and see cartilage in three dimensions. Some people with OA have lesions similar to Bone Marrow Edema (BME), which significantly challenge automated cartilage segmentation. In patients with and without bone anomalies, automated knee cartilage segmentation using the modified radial approach was shown to be feasible, as reported by R. Thaha *et al*. [126]. The primary purpose of this investigation was to design an automated segmentation method that would be successful in healthy persons as well as OA patients with and without BME lesions. We devised an automated technique for segmenting cartilage by using T2 map data and a modified radial methodology. The coefficients of similarity were used to conduct an analysis that determined how accurate the suggested method was. Twelve MRI datasets were successfully segregated by making use of the strategy that was provided.

An approach to bone segmentation in MDCT images for the knee joint was suggested by Y. Uozumi *et al*. [127]. In this particular investigation, the femur, tibia, patella, and fibular bones of the knee are each manually and mechanically dissected into their respective segments. In a study, it was tested on six persons aged 33 to 13, and the results were analyzed (four men and two women). There is a rationale in terms of anatomy to the practice of dissecting the knee joint into its component bones. In the course of the testing, both the validity of the manual's matching rate and the most effective technique for determining that rate were examined and tested.

The matching rates of the femur, tibia, patella, and fibula were thus 95.84±0.57%, 94.12±1.01%, 94.49±0.83%, and 86.37±4.28%, respectively. This investigation concluded that the approach suggested is sufficient to segment the knee bones. Researchers were successful in separating the bones in the knee by employing this technique.

Ultrasonography, sometimes known as US, is a diagnostic tool that may be used in the early stages of osteoarthritis of the knee in order to evaluate the degree of cartilage damage (OA).

A framework for the automatic segmentation of knee cartilage from improved US images has been provided by P. R. Desai *et al*. [128]. The augmentation of bone surfaces is facilitated by calculating local phase image characteristics included in the proposed framework. The dynamic programming method is used to segment the bones, and the surface areas of the segmented bones are used as seeds in the random walker method. Eight healthy participants participated in the research and submitted a total of one hundred scans. Eight scans were used for the validation study's qualitative and quantitative analyses. The validation results against an expert's manual segmentation yielded a DSC of 0.8758 on average.

An efficient classification approach for knee MR image segmentation was developed by Y. Yamamoto *et al*. [129]. Using the evolutionary categorization system CBGA-LDIC, MR images of the knee bone may be automatically recognized. CBGA-LDIC is used to identify an efficient cell set for image segmentation. In order to identify photographs in terms of the geographic place to which they were taken, LDIC is combined with a genetic algorithm, also known as GA, and case-based reasoning (CB). Segmenting pictures using LDIC's one-of-a-kind yet locally applicable approaches and several location-dependent classifiers is now possible. Every single classifier is educated with the help of a Gaussian mixture model.

CBGA-LDIC decomposes an image into its component pixels to generate a collection of pixels and then trains classifiers on those constructed collections. As a result of the proximity of the knee bones to one another and/or the similarities in the form of the bones themselves, favorable combinations of cells are preserved in case of bases for later customers. If favorable cell combinations are identified in patients just beginning the GA process, then this method ought to provide superior outcomes. The results of several of the experiments described in this section lend credence to this assertion.

S. Suresha *et al*. [130] demonstrate how to stage the severity of knee osteoarthritis using open-source software that utilizes X-ray pictures and completely automated open-source technology. Despite recent advances in machine learning, particularly in the field of deep learning, the automated interpretation of X-ray and MRI data continues to be a key bottleneck in the study of osteoarthritis. This is particularly true in the United States. Research on osteoarthritis might benefit from the recent developments in deep learning, which could be applied to the database maintained by the Osteoarthritis Initiative (OAI). The author has shown that deep learning algorithms may be utilized to automate the severity staging of knee osteoarthritis using X-ray data.

This was accomplished by analyzing the images produced by X-ray machines. For this particular study, the author used a total of 7549 X-ray images of knees in fixed flexion—both the right and the left—that had previously been assessed on the Kellgren-Lawrence (KL) scale by qualified radiologists. During the testing phase, just 25% of the data were used, while the remaining data were included in the model. This step culminated in the division of this set into sets for training and testing. In order to accomplish the two goals detailed below, the author constructed a region convolutional neural network using a deep neural network in a very short amount of time. (1) extract the knee-joint region from the X-ray images and (2) classify the knee-joint regions using the KL scale (0e4).

G.B. Joseph *et al*. [133 - 137] determine whether or not preliminary T2 relaxation time measurements of knee cartilage in individuals who have risk factors for osteoarthritis are linked to the progression of cartilage, meniscus, and bone tissue degeneration over the course of three years, these measurements will be studied (OA). The Osteoarthritis Initiative (OAI) database allowed for identifying 289 individuals who exhibited OA risk factors (45±55 years of age). The researchers used the scores obtained from a 3.0 Tesla MR scan to assess the overall health of the menisci and cartilage (WORMS scoring).

A method called “T2 mapping” was used to determine the average and heterogeneity of T2 (gray-level co-occurrence matrix texture analysis). Researchers utilized regression models to investigate whether or if there was a correlation between the three-year changes in morphological knee WORMS scores and the baseline T2 levels.

For the clinical manifestations of osteoarthritis, an investigation into the use of pixel-based segmentation and the SVM classifier was provided by Bhagyashri L *et al*. [132]. Pixel-based image segmentation and the Support Vector Machine (SVM) classifier are diagnostic tools that may be used in osteoarthritis diagnosis (OA). During this procedure, MRI scans are performed on the joint areas of the knee. Segmenting cartilage into its component parts is feasible using several image processing methods, including thresholding and noise reduction. When determining statistical and form features, parts of an image's texture are used as inputs. These qualities include colour and shape. These characteristics are used in the training of the SVM, and the results are classified as either normal or influenced by OA.

Osteoarthrosis (OA) is a multi-factorial disease characterized by the progressive loss of articular cartilage and the development of subchondral sclerosis, intra-osseous cysts and osteophytes. In addition to changes in cartilage that occur in OA, it is suggested that early changes are seen in the adjoining subchondral and trabecular bone.

Table 8. Typical Thickness Measurement Methods.

Authors	2D/3D	Method	Weakness
Solloway *et al*. [111].	2D	'M-Norm'	1. The distance defined in 2D space could not accurately reflect the true thickness; 2. The method is unstable.
Tang *et al*. [110].	2D	'T-norm.'	The distance defined in 2D space could not accurately reflect the true thickness.
Cohen *et al*. [106].	3D	Ray casting.	The method is unstable when the BCI is not smooth.
Fripp *et al*. [35]. Stammberger *et al*. [134, 135]. Carballido-Gamio *et al*. [108, 109].	3D	3D Euclidean distance transformation.	High computational cost.
Williams *et al*. [62, 136].	3D	'Spans and Ridges.'	The method BCI is not smooth and is unstable when the
Shan *et al*. [42, 73], Huang *et al*. [121].	3D	3D Laplace-equation.	High computational cost.
Kauffmann *et al*. [137].	3D	Thickness map	High computational cost

Characterization of trabecular bone micro-architecture in the knee in osteoarthrosis using high-resolution MRI paper presented by O. Beuf *et al*. [133 - 148]. In this work, the author develops, optimizes and extends MR techniques to depict and quantify trabecular bone structure *in vivo* in the knee joint, in the distal femur and proximal tibia. Authors characterize and quantify the variations of the trabecular bone structure measures along the distal femur and proximal tibia and examine the difference in trabecular structure between the tibia and femur in joints unaffected and affected by OA.

3. TYPICAL THICKNESS MEASUREMENT METHODS

The researchers and clinicians must develop a different approach to measure the thickness of knee bone and cartilage to assess knee osteoarthritis. It is very important for the medical practitioner to perform a volumetric analysis of segmented parts in order to analyze the different stages of OA. Many researchers have developed various methods for morphological assessment and quantifying different knee joints. Table **8** provides the summary of different thickness measurement methods proposed by various researchers on knee joints using MR Images.

4. DISCUSSION

The semi-automatic and fully-automatic segmentation of different parts of knee joints has evolved as a critical area of research in the last two decades. This literature review outlined various conventional and recently developed deep-learning methods for bone, cartilage, and meniscus segmentation and quantification. The studies involved MR Images as a diagnostic tool as MR images provide more detailed information on the anatomical position of menisci and surrounding tissues. Additionally, performing MR scans is non-invasive, ensuring less patient discomfort. The study includes subchondral bone segmentation and quantifies modifications in the tibial plateau, bony surface contour (*e.g.*, subchondral bone attrition), bone shape, surface geometry, and area from a 3D model reconstructed from segmented bone regions as an imaging biomarker to track the progression of knee OA. Various researchers have proposed semi-automated and fully automated techniques for the segmentation of morphological features of bone, such as Active Shape Models (ASM), Active Appearance Models (AAM), Statistical Shape Models (SSM), classification techniques (*e.g.*, voxel, phase, or texture), and atlas-based methods. Fully automatic segmentation methods are also more sensitive and produce the best results. It has also been discovered that fully automatic segmentation methods are more sensitive and deliver the best results. When datasets or training samples change, the flexibility of the developed process in the global domain is reduced. Although many automatic segmentation techniques are available in the literature, there is still much room for research in this field because many available methods have gaps, as discussed in the preceding review. The segmentation techniques help clinicians and rheumatologists to detect and diagnose various abnormal conditions in the bone in the early phase of the disease. Several deep learning-based methods have recently been proposed that outperform the conventional knee joint segmentation methods.

Deep learning-based models overcome various drawbacks present in traditional techniques in terms of accurate segmentation of knee bone.

Articular cartilage segmentation is a critical and challenging task due to its shape, irregularity, and connection with surrounding tissues. The quantification of knee AC assists clinicians in diagnosing osteoarthritis at various stages. Several studies have been conducted over a long period to segment AC, which helps to detect the condition of patients suffering from OA. Many conventional automatic and semi-automatic techniques, such as Optimization of Local Shape and Appearance, KNN classification, Multi-contrast MR and Classification, 3D Statistical Shape Models (SSMs), and so on, are used by the researcher to segment the AC from MR Images accurately. Most techniques are learning-based, necessitating a large amount of training data at first, and even minor changes in the training data can affect the possible outcomes.

It also takes the same time as it did at the beginning of training for every small change in data. This opens up

opportunities for researchers to contribute to this field by developing efficient techniques in terms of both time and computations while also having high sensitivity, specificity, and DSC. Because they are computationally expensive, DL-based segmentation techniques can achieve acceptable overall performance compared to atlas-based and model-based methods. As a result, researchers are encouraged to use combined DL-based models and any other strategy that can achieve higher accuracy levels than those reported in previous studies. Compared to UNet and LOGISMOS on their own, the combination of UNet and LOGISMOS improved pancreas segmentation significantly.

Because of its capacity to absorb shock and distribute the load, the meniscus is essential to a healthy knee joint. Meniscal damage is a common finding on an osteoarthritic knee MRI. Nonetheless, a small group of researchers pioneered automatic segmentation of knee menisci during the current decade, regarded as a cornerstone in this field. It inspired others to use machine learning algorithms to perform segmentation. Fully automated segmentation involves Shape based segmentation. Image-based segmentation provides excellent segmentation results in comparison with the manual approach. This helps majorly in treating meniscus tears and morphological changes, which can cause damage to the knee meniscus. Recently many researchers have also proposed a machine learning and deep learning-based approach to increase segmentation accuracy. Thereby it helps quantify and visualize the meniscus to determine the affected areas.

From this review, it is observed that researchers initially emphasized Semi-Automatic segmentation over Manual methods where for inputs and for processing the images, users were needed. Later, the researcher switched to fully-automated ways, where segmentation accuracy was outstanding compared to semi-automated methods and reduced human involvement. Deep learning-based methods with minimal user input have recently been used to perform automatic segmentation. U-Net, VGG Net, Segnet, and ATTU-Net, a convolutional network based on graphics processing units (GPUs) developed for biomedical image segmentation, were used in the studies. Applying deep learning methods in medical imaging provides various research issues, allowing the researcher to focus and conduct their research. We have comprehensively reviewed different segmentation and quantifying methods focusing on crucial parts of the knee joint such as bone, Articular Cartilage and Meniscus.

CONCLUSION

This comprehensive review article aims to provide complete insight into various segmentation and quantification techniques emphasizing Knee bone, Articular Cartilage and meniscus, as these are the critical parts for knee damages and impairments. The review provides a detailed explanation of conventional semi-automated and fully-automated segmentation techniques, which helps in many clinical applications. In addition, we have reviewed current DL-based methods for segmentation and quantification using MR Images, which creates many opportunities for researchers and clinicians to detect the damages present in the knee joint in the early stages.

LIST OF ABBREVIATIONS

MRI	=	Magnetic Resonance Imaging
OA	=	Osteoarthritis
AC	=	Articular Cartilage
AC	=	Anterior Compartment
DSC	=	Dice Similarity Coefficient

CONSENT FOR PUBLICATION

Not applicable.

FUNDING

None.

CONFLICT OF INTEREST

The authors declare no conflicts of interest, financial or otherwise.

ACKNOWLEDGEMENTS

Declared none.

REFERENCES

[1] Castañeda S, Roman-Blas JA, Largo R, Herrero-Beaumont G. Subchondral bone as a key target for osteoarthritis treatment. Biochem Pharmacol 2012; 83(3): 315-23. [http://dx.doi.org/10.1016/j.bcp.2011.09.018] [PMID: 21964345]

[2] Gait AD, Hodgson R, Parkes MJ, *et al.* Synovial volume *vs* synovial measurements from dynamic contrast enhanced MRI as measures of response in osteoarthritis. Osteoarthritis Cartilage 2016; 24(8): 1392-8. [http://dx.doi.org/10.1016/j.joca.2016.03.015] [PMID: 27038489]

[3] Bowes MA, Vincent GR, Wolstenholme CB, Conaghan PG. A novel method for bone area measurement provides new insights into osteoarthritis and its progression. Ann Rheum Dis 2013; 74(3): 519-25.

[4] Hunter D, Nevitt M, Lynch J, *et al.* Longitudinal validation of periarticular bone area and 3D shape as biomarkers for knee OA progression? Data from the FNIH OA Biomarkers Consortium. Ann Rheum Dis 2015; 75(9): 1607-4.

[5] Neogi T, Felson DT. Bone as an imaging biomarker and treatment target in OA. Nat Rev Rheumatol 2016; 12(9): 503-4. [http://dx.doi.org/10.1038/nrrheum.2016.113] [PMID: 27383914]

[6] Heimann T. Segmentation of knee images: A grand challenge. Proc MICCAIWorkshop on Medical Image Analysis for the Clinic 2010.

[7] Carmen Taylor J. Comparison of quantitative imaging of cartilage for osteoarthritis: T2, T1ρ, dGEMRIC, and contrast-enhanced CT. Magn Reson Imaging 2009; 27(6): 779-84. [http://dx.doi.org/10.1016/j.mri.2009.01.016] [PMID: 19269769]

[8] Neogi T, Bowes MA, Niu J, *et al.* Magnetic resonance imaging-based three-dimensional bone shape of the knee predicts onset of knee osteoarthritis: data from the osteoarthritis initiative. Arthritis Rheum 2013; 65(8): 2048-58. [http://dx.doi.org/10.1002/art.37987] [PMID: 23650083]

[9] MacKay JW, *et al.* Subchondral bone in osteoarthritis: Association between MRI texture analysis and histomorphometry. Osteoarthritis Cartilage 2016. [PMID: 27986620]

[10] Ababneh SY, Prescott JW, Gurcan MN. Automatic graph-cut based segmentation of bones from knee magnetic resonance images for osteoarthritis research. Med Image Anal 2011; 15(4): 438-48. [http://dx.doi.org/10.1016/j.media.2011.01.007] [PMID: 21474362]

[11] Jose Gerardo Tamez-Pena ST. Performance assessment of an automated segmentation system for knee MRI scans. ORS 2016.

[12] Dam EB, Lillholm M, Marques J, Nielsen M. Automatic segmentation of high- and low-field knee MRIs using knee image quantification with data from the osteoarthritis initiative. J Med Imaging (Bellingham) 2015; 2(2): 024001-1. [http://dx.doi.org/10.1117/1.JMI.2.2.024001] [PMID: 26158096]

[13] Dodin P, Martel-Pelletier J, Pelletier JP, Abram F. A fully automated human knee 3D MRI bone segmentation using the ray casting technique. Med Biol Eng Comput 2011; 49(12): 1413-24. [http://dx.doi.org/10.1007/s11517-011-0838-8] [PMID: 22038239]

[14] Balsiger F, Ronchetti T, Pletscher M. Distal femur segmentation on MR images using random forests. Medical Image Analysis Laboratory 2015.

[15] Wang Q. Semantic context forests for learning-based knee cartilage segmentation in 3D MR images. International MICCAI Workshop on Medical Computer Vision 2013.

[16] Bindernagel M, Kainmueller D, Seim H, Lamecker H, Zachow S, Hege HC. An articulated statistical shape model of the human knee. In: Bildverarbeitung für die Medizin 2011. Berlin, Heidelberg: Springer 2011; pp. 59-63. [http://dx.doi.org/10.1007/978-3-642-19335-4_14]

[17] Seim H, Kainmueller D, Lamecker H, Bindernagel M, Malinowski J, Zachow S. Model-based Auto-Segmentation of Knee Bones and Cartilage in MRI Data. Auto-Segmentation of the Knee in MRI Data 2010.

[18] Shan L, Zach C, Styner M, Charles C, Niethammer M. Automatic Bone Segmentation and Alignment From MR Knee Images. Proceedings of SPIE - The International Society for Optical Engineering 2010. [http://dx.doi.org/10.1117/12.841167]

[19] Ratzlaff C, Guermazi A, Collins J, *et al.* A rapid, novel method of volumetric assessment of MRI-detected subchondral bone marrow lesions in knee osteoarthritis. Osteoarthritis Cartilage 2013; 21(6): 806-14. [http://dx.doi.org/10.1016/j.joca.2013.03.007] [PMID: 23518154]

[20] Deniz CM, Xiang S, Hallyburton RS, *et al.* Segmentation of the Proximal Femur from MR Images using Deep Convolutional Neural Networks. Sci Rep 2018; 8(1): 16485. [http://dx.doi.org/10.1038/s41598-018-34817-6] [PMID: 30405145]

[21] Kim D, Lee J, Yoon JS, Lee KJ, Won K. Development of automated 3D knee bone segmentation with inhomogeneity correction for deformable approach in magnetic resonance imaging. RACS '18: Proceedings of the 2018 Conference on Research in Adaptive and Convergent Systems 2018; 285-90. [http://dx.doi.org/10.1145/3264746.3264776]

[22] Zhou Z, Zhao G, Kijowski R, Liu F. Deep convolutional neural network for segmentation of knee joint anatomy. Magn Reson Med 2018; 80(6): 2759-70. [http://dx.doi.org/10.1002/mrm.27229] [PMID: 29774599]

[23] Roemer F, Neogi T, Nevitt M, *et al.* Subchondral bone marrow lesions are highly associated with, and predict subchondral bone attrition longitudinally: the MOST study. Osteoarthritis Cartilage 2009; 18(1): 47.

[24] Tiulpin A, Thevenot J, Rahtu E, Lehenkari P, Saarakkala S. Automatic knee osteoarthritis diagnosis from plain radiographs: A deep learning-based approach. Sci Rep 2018; 8(1): 1727. [http://dx.doi.org/10.1038/s41598-018-20132-7] [PMID: 29379060]

[25] Ambellan F, Tack A, Ehlke M, Zachow S. Automated segmentation of knee bone and cartilage combining statistical shape knowledge and convolutional neural networks: Data from the Osteoarthritis Initiative. Med Image Anal 2019; 52: 109-18. [http://dx.doi.org/10.1016/j.media.2018.11.009]

[26] Schock J. A method for semantic knee bone and cartilage segmentation with deep 3D shape fitting using data from the osteoarthritis initiative. Shape in Medical Imaging ShapeMI 2020 Lecture Notes in Computer Science 2020; 12474

[27] Rini C, Perumal B, Rajasekaran MP. Automatic knee joint segmentation using Douglas-Rachford splitting method. Multimedia Tools Appl 2020; 79(9-10): 6599-621. [http://dx.doi.org/10.1007/s11042-019-08303-8]

[28] Gatti AA, Maly MR. Automatic knee cartilage and bone segmentation using multi-stage convolutional neural networks: data from the osteoarthritis initiative. MAGMA 2021; 34(6): 859-75. [http://dx.doi.org/10.1007/s10334-021-00934-z] [PMID: 34101071]

[29] Heckelman LN, Soher BJ, Spritzer CE, Lewis BD, DeFrate LE. Design and validation of a semi-automatic bone segmentation algorithm from MRI to improve research efficiency. Sci Rep 2022; 12(1): 7825. [http://dx.doi.org/10.1038/s41598-022-11785-6] [PMID: 35551485]

[30] Rini C, Perumal B, Pallikonda Rajasekaran M, Muneeswaran V. Automatic knee segmentation using eagle algorithm with multi stochastic objective process. 3C Tecnología 2021; 2021: 333-53. [http://dx.doi.org/10.17993/3ctecno.2021.specialissue8.333-353]

[31] Robert B, Boulanger P. Automatic Bone Segmentation from MRI for Real-Time Knee Tracking in Fluoroscopic Imaging. Diagnostics (Basel) 2022; 12(9): 2228. [http://dx.doi.org/10.3390/diagnostics12092228] [PMID: 36140633]

[32] Patekar R, Kumar PS, Gan H-S, Ramlee MH. Automated knee bone segmentation and visualisation using mask RCNN and marching cube: Data from the osteoarthritis initiative. ASM Science Journal 2022.

[33] Gandhamal A, Talbar S, Gajre S, Razak R, Hani AFM, Kumar D. Fully automated subchondral bone segmentation from knee MR images: Data from the Osteoarthritis Initiative. Comput Biol Med 2017; 88: 110-25. [http://dx.doi.org/10.1016/j.compbiomed.2017.07.008] [PMID: 28711767]

[34] Chen H, Zhao N, Tan T, *et al.* Knee Bone and Cartilage Segmentation Based on a 3D Deep Neural Network Using Adversarial Loss for Prior Shape Constraint. Front Med (Lausanne) 2022; 9: 792900. [http://dx.doi.org/10.3389/fmed.2022.792900] [PMID: 35669917]

[35] Fripp J, Crozier S, Warfield SK, Ourselin S. Automatic segmentation of the bone and extraction of the bone–cartilage interface from magnetic resonance images of the knee. Phys Med Biol 2007; 52(6): 1617-31. [http://dx.doi.org/10.1088/0031-9155/52/6/005] [PMID: 17327652]

[36] Folkesson J, Dam EB, Olsen OF, Pettersen PC, Christiansen C. Segmenting articular cartilage automatically using a voxel classification approach. IEEE Trans Med Imaging 2007; 26(1): 106-15. [http://dx.doi.org/10.1109/TMI.2006.886808] [PMID: 17243589]

[37] Wu D, Sofka M, Birkbeck N, Zhou SK. Segmentation of multiple knee bones from CT for orthopedic knee surgery planning. Med Image Comput Comput Assist Interv 2014; 17(Pt 1): 372-80. [http://dx.doi.org/10.1007/978-3-319-10404-1_47]

[38] Lee S, Park SH, Shim H, Yun ID, Lee SU. Optimization of local shape and appearance probabilities for segmentation of knee cartilage in 3-D MR images. Comput Vis Image Underst 2011; 115(12): 1710-20. [http://dx.doi.org/10.1016/j.cviu.2011.05.014]

[39] Liang S, Charles C, Niethammer M. Automatic multi-atlas-based cartilage segmentation from knee MR images. Biomedical Imaging 2012; 1028-31.

[40] Zhang K, Lu W, Marziliano P. Automatic knee cartilage segmentation from multi-contrast MR images using support vector machine classification with spatial dependencies. Magn Reson Imaging 2013; 31(10): 1731-43. [http://dx.doi.org/10.1016/j.mri.2013.06.005]

[41] Lee J-G, Gumus S, Moon C-H, Kwoh K, Bae KT. Fully automated segmentation of cartilage from the MR images of knee using a multi-atlas and local structural analysis method. Med Phys 2014; 41(9): 092303. [http://dx.doi.org/10.1118/1.4893533]

[42] Shan L, Zach C, Charles C, Niethammer M. Automatic atlas-based three-label cartilage segmentation from MR knee images. Med Image Anal 2014; 18(7): 1233-46. [http://dx.doi.org/10.1016/j.media.2014.05.008] [PMID: 25128683]

[43] Pang J, Li P, Qiu M, Chen W, Qiao L. Automatic Articular Cartilage Segmentation Based on Pattern Recognition from Knee MRI Images. J Digit Imaging 2015; 28(6): 695-703. [http://dx.doi.org/10.1007/s10278-015-9780-x] [PMID: 25700618]

[44] Öztürk CN, Albayrak S. Automatic segmentation of cartilage in high-field magnetic resonance images of the knee joint with an improved voxel-classification-driven region-growing algorithm using vicinity-correlated subsampling. Comput Biol Med 2016; 72: 90-107. [http://dx.doi.org/10.1016/j.compbiomed.2016.03.011] [PMID: 27017069]

[45] Alderin F. Automated Segmentation of the Meniscus. Examination work within the field of technology medical technology and the main area engineering physics, advanced level, 30 HP Stockholm, Sweden. 2017.

[46] Norman B, Pedoia V, Majumdar S. Use of 2D U-Net Convolutional Neural Networks for Automated Cartilage and Meniscus Segmentation of Knee MR Imaging Data to Determine Relaxometry and Morphometry. Radiology 2018; 288(1): 177-85. [http://dx.doi.org/10.1148/radiol.2018172322] [PMID: 29584598]

[47] Dodin P, Abram F, Pelletier JP, Martel-Pelletier J. A fully automated system for quantification of knee bone marrow lesions using MRI and the osteoarthritis initiative cohort. J Biomed Graph Comput 2012; 3(1): 51-65. [http://dx.doi.org/10.5430/jbgc.v3n1p51]

[48] Ahn C, Bui TD, Lee Y, Shin J, Park H. Fully automated, level set-based segmentation for knee MRIs using an adaptive force function and template: data from the osteoarthritis initiative. Biomed Eng Online 2016; 15(1): 99. [http://dx.doi.org/10.1186/s12938-016-0225-7] [PMID: 27558127]

[49] Brui E, Efimtcev AY, Fokin VA, *et al.* Deep learning-based fully automatic segmentation of wrist cartilage in MR images. NMR Biomed 2020; 33(8): e4320. [http://dx.doi.org/10.1002/nbm.4320] [PMID: 32394453]

[50] Liu F, Zhou Z, Samsonov A, *et al.* Deep learning approach for evaluating knee MR images: Achieving high diagnostic performance for cartilage lesion detection. Radiology 2018; 289(1): 160-9. [http://dx.doi.org/10.1148/radiol.2018172986] [PMID: 30063195]

[51] Liu F, Zhou Z, Jang H, Samsonov A, Zhao G, Kijowski R. Deep convolutional neural network and 3D deformable approach for tissue segmentation in musculoskeletal magnetic resonance imaging: Deep Learning Approach for Segmenting MR Image. Magn Reson Med 2018. 79(2). [http://dx.doi.org/10.1002/mrm.26841]

[52] Liu F. SUSAN: Segment unannotated image structure using adversarial network. Magn Reson Med 2019; 81(5): 3330-45. [PMID: 30536427]

[53] Kashyap S, Zhang H, Sonka M. Just-enough interaction approach to knee MRI segmentation: Data from the osteoarthritis initiative. arXiv:190304027v1 2019.

[54] Bonaretti S, Gold GE, Beaupre GS. pyKNEEr: An image analysis workflow for open and reproducible research on femoral knee cartilage. PLoS One 2019; 15(1): e0226501.

[55] Kashyap S, Oguz I, Zhang H, Sonka M. Automated segmentation of knee MRI using hierarchical classifiers and just enough interaction based learning: Data from osteoarthritis initiative. Medical Image Computing and Computer-Assisted Intervention – MICCAI 2016 MICCAI 2016 Lecture Notes in Computer Science 2019; 9901

[56] Kashyap S, Zhang H, Rao K, Sonka M. Learning-based cost functions for 3D and 4D multi-surface multi-object segmentation of Knee MRI: Data from the osteoarthritis initiative. IEEE Transactions on Medical Imaging 2018; 37(5): 1103-13. [http://dx.doi.org/10.1109/TMI.2017.2781541]

[57] Fripp J, Crozier S, Warfield SK, Ourselin S. Automatic segmentation and quantitative analysis of the articular cartilages from magnetic resonance images of the knee. IEEE Trans Med Imaging 2010; 29(1): 55-64. [http://dx.doi.org/10.1109/TMI.2009.2024743] [PMID: 19520633]

[58] Dodin P, Pelletier J, Martel-Pelletier J, Abram F. Automatic Human Knee Cartilage Segmentation From 3-D Magnetic Resonance Images. IEEE Trans Biomed Eng 2010; 57(11): 2699-711. [http://dx.doi.org/10.1109/TBME.2010.2058112]

[59] Ali Shah SA, Yahya KM, Mubashar G, Bais A. Quantification and visualization of MRI cartilage of the knee: A simplified approach. 2010 6th International Conference on Emerging Technologies (ICET) 2010. [http://dx.doi.org/10.1109/ICET.2010.5638495]

[60] Mallikarjuna Swamy MS, Holi MS. Knee joint cartilage visualization and quantification in normal and osteoarthritis. 2010 International Conference on Systems in Medicine and Biology 2010. [http://dx.doi.org/10.1109/ICSMB.2010.5735360]

[61] Long NQ, Jiang D, Ding C. "Application of artificial neural networks in automatic cartilage segmentation," 3rd Int. Work Adv Comput Intell IWACI 2010; 2010: 81-5.

[62] Williams TG. Automatic segmentation of bones and inter-image anatomical correspondence by volumetric statistical modelling of knee MRI. 2010 IEEE International Symposium on Biomedical Imaging: From Nano to Macro 2010. [http://dx.doi.org/10.1109/ISBI.2010.5490316]

[63] Yin Yin , Xiangmin Zhang , Williams R, Xiaodong Wu , Anderson DD, Sonka M. Logismos layered optimal graph image segmentation of multiple objects and surfaces: Cartilage segmentation in the knee joint. IEEE Trans Med Imaging 2010; 29(12): 2023-37. [http://dx.doi.org/10.1109/TMI.2010.2058861] [PMID: 20643602]

[64] Tamez-Pena J, González P, Farber J, Baum K, Schreyer E, Totterman S. Atlas based method for the automated segmentation and quantification of knee features: Data from the osteoarthritis initiative Int Symp Biomed Imaging 1484-7.2011; [http://dx.doi.org/10.1109/ISBI.2011.5872681]

[65] Zhang K, Deng J, Lu W. Segmenting human knee cartilage automatically from multi-contrast MR images using support vector machines and discriminative random fields. 2011 18th IEEE International Conference on Image Processing 2011. [http://dx.doi.org/10.1109/ICIP.2011.6116655]

[66] Jiang J-G. Segmentation of knee joints based on improved multiphase Chan-Vese model. 2008 2nd International Conference on Bioinformatics and Biomedical Engineering 2008.

[67] Marstal K, Gudbergsen H, Boesen M, Kubassova O, Bouert R, Bliddal H. Semi-automatic segmentation of knee osteoarthritic cartilage in magnetic resonance images. Proceedings ELMAR-2011 2011; 385-8.

[68] Tran HV, Jiang D. Articular cartilage segmentation in noisy MR images of human knee 2012 Cairo International Biomedical Engineering Conference (CIBEC). 146-9. [http://dx.doi.org/10.1109/CIBEC.2012.6473331]

[69] Tamez-Peña JG, Farber J, González PC, Schreyer E, Schneider E, Totterman S. Unsupervised segmentation and quantification of anatomical knee features: data from the Osteoarthritis Initiative. IEEE Trans Biomed Eng 2012; 59(4): 1177-86. [http://dx.doi.org/10.1109/TBME.2012.2186612] [PMID: 22318477]

[70] Kashyap S, Yin Y, Sonka M. Automated analysis of cartilage morphology 2013 IEEE 10th International Symposium on Biomedical Imaging. 1300-3.

[71] Prasoon A, Petersen K, Igel C, Lauze F, Dam E, Nielsen M. Deep feature learning for knee cartilage segmentation using a triplanar convolutional neural network. International conference on medical image computing and computer-assisted intervention 2013; 246-53. [http://dx.doi.org/10.1007/978-3-642-40763-5_31]

[72] Prasoon A, Igel C, Loog M, Lauze F, Dam EB, Nielsen M. Femoral cartilage segmentation in Knee MRI scans using two stage voxel classification. 2013 35th Annual International Conference of the IEEE Engineering in Medicine and Biology Society (EMBC) 2013. [http://dx.doi.org/10.1109/EMBC.2013.6610787]

[73] Shan L, Charles C, Niethammer M. Longitudinal three-label segmentation of knee cartilage. 2013 IEEE 10th International Symposium on Biomedical Imaging 2013.

[74] Gan HS, Tan TS, Sayuti KA, Karim AHA, Kadir MRA. Multilabel graph based approach for knee cartilage segmentation: Data from the osteoarthritis initiative. 2014 IEEE Conference on Biomedical Engineering and Sciences (IECBES). 210-3. [http://dx.doi.org/10.1109/IECBES.2014.7047487]

[75] Kubicek J, Penhaker M. Fuzzy algorithm for segmentation of images in extraction of objects from MRI. 2014 International Conference on Advances in Computing, Communications and Informatics (ICACCI) 2014; 1422-7. [http://dx.doi.org/10.1109/ICACCI.2014.6968264]

[76] Gan HS. Binary Seeds Auto Generation Model for Knee Cartilage Segmentation. 2018 International Conference on Intelligent and Advanced System (ICIAS) 2018. [http://dx.doi.org/10.1109/ICIAS.2018.8540570]

[77] Revathi SA, Holi G. Cartilage Segmentation of Knee OsteoArthritis from Magnetic Resonance Images(MRI). 2018 Second International Conference on Advances in Electronics, Computers and Communications (ICAECC) 2018.

[78] Viken H, Angman M. Automatic segmentation of articular cartilage in arthroscopic images using deep neural networks and multifractal analysis. Linköping University Department of Biomedical Engineering Master's thesis, 30 ECTS Computer science. 2020.

[79] Xue YP, Jang H, Byra M, *et al.* Automated cartilage segmentation and quantification using 3D ultrashort echo time (UTE) cones MR imaging with deep convolutional neural networks. Eur Radiol 2021; 31(10): 7653-63. [http://dx.doi.org/10.1007/s00330-021-07853-6] [PMID: 33783571]

[80] Dimitri A, MacKay JW, McDonnell SM, *et al.* Segmentation of knee MRI data with convolutional neural networks for semi-automated three-dimensional surface-based analysis of cartilage morphology and composition. Osteoarthritis Imaging 2022; 2(2): 100010.

[81] Yang M, Colak C, Chundru KK, *et al.* Automated knee cartilage segmentation for heterogeneous clinical MRI using generative adversarial networks with transfer learning. Quant Imaging Med Surg 2022; 12(5): 2620-33. [http://dx.doi.org/10.21037/qims-21-459] [PMID: 35502381]

[82] Stehling C, Baum T, Mueller-Hoecker C, *et al.* A novel fast knee cartilage segmentation technique for T2 measurements at MR imaging – data from the Osteoarthritis Initiative. Osteoarthritis Cartilage 2011; 19(8): 984-9. [http://dx.doi.org/10.1016/j.joca.2011.04.002] [PMID: 21515391]

[83] Frondelius T, Tiulpin A, Lehenkari P, Nieminen HJ, Saarakkala S. Fully automatic deep learning based segmentation of bone-cartilage interface from micro-CT images of human osteochondral samples. Osteoarthr Cartil 2018; 26(1): S469. [http://dx.doi.org/10.1016/j.joca.2018.02.885]

[84] Wirth W, Maschek S, Beringer P, Eckstein F. Subregional laminar cartilage MR spin–spin relaxation times (T2) in osteoarthritic knees with and without medial femorotibial cartilage loss – data from the

Osteoarthritis Initiative (OAI). Osteoarthr Cartil 2017; 25(8): 1313-23. [http://dx.doi.org/10.1016/j.joca.2017.03.013] [PMID: 28351705]

[85] Si Liping, Xuan Kai, Zhong Jingyu, *et al.* Knee cartilage thickness differs alongside ages: A 3-T magnetic resonance research upon 2,481 subjects *via* deep learning. Front Med 2021; 7: 600049. [http://dx.doi.org/10.3389/fmed.2020.600049]

[86] Almajalid R, Shan J, Du Y, Zhang M. Identification of Knee Cartilage Changing Pattern. Appl Sci (Basel) 2019; 9(17): 3469. [http://dx.doi.org/10.3390/app9173469]

[87] Panfilov Egor. Deep learning-based segmentation of knee MRI for fully automatic subregional morphological assessment of cartilage tissues: Data from the osteoarthritis initiative. J Orthop Res 2021; 40(5): 1113-24.

[88] Sekiya I, Kohno Y, Hyodo A, *et al.* Interscan measurement error of knee cartilage thickness and projected cartilage area ratio at 9 regions and 45 subregions by fully automatic three-dimensional MRI analysis. Eur J Radiol 2021; 139: 109700. [http://dx.doi.org/10.1016/j.ejrad.2021.109700] [PMID: 33865065]

[89] Englund M, Guermazi A, Roemer FW, *et al.* Meniscal tear in knees without surgery and the development of radiographic osteoarthritis among middle-aged and elderly persons: The multicenter osteoarthritis study. Arthritis Rheum 2009; 60(3): 831-9. [http://dx.doi.org/10.1002/art.24383] [PMID: 19248082]

[90] Hunter DJ, Zhang YQ, Niu JB, *et al.* The association of meniscal pathologic changes with cartilage loss in symptomatic knee osteoarthritis. Arthritis Rheum 2006; 54(3): 795-801. [http://dx.doi.org/10.1002/art.21724] [PMID: 16508930]

[91] Sharma L, Eckstein F, Song J, *et al.* Relationship of meniscal damage, meniscal extrusion, malalignment, and joint laxity to subsequent cartilage loss in osteoarthritic knees. Arthritis Rheum 2008; 58(6): 1716-26. [http://dx.doi.org/10.1002/art.23462] [PMID: 18512777]

[92] Paproki A, Engstrom C, Chandra SS, Neubert A, Fripp J, Crozier S. Automated segmentation and analysis of normal and osteoarthritic knee menisci from magnetic resonance images – data from the Osteoarthritis Initiative. Osteoarthritis Cartilage 2014; 22(9): 1259-70. [http://dx.doi.org/10.1016/j.joca.2014.06.029] [PMID: 25014660]

[93] Tack A, Mukhopadhyay A, Zachow S. Knee menisci segmentation using convolutional neural networks: data from the Osteoarthritis Initiative. Osteoarthritis Cartilage 2018; 26(5): 680-8. [http://dx.doi.org/10.1016/j.joca.2018.02.907] [PMID: 29526784]

[94] Bloecker K, Wirth W, Hudelmaier M, Burgkart R, Frobell R, Eckstein F. Morphometric differences between the medial and lateral meniscus in healthy men - a three-dimensional analysis using magnetic resonance imaging. Cells Tissues Organs 2012; 195(4): 353-64. [http://dx.doi.org/10.1159/000327012] [PMID: 21709397]

[95] Zarandi MHF, Khadangi A, Karimi F, Turksen IB. A Computer-Aided Type-II Fuzzy Image Processing for Diagnosis of Meniscus Tear. J Digit Imaging 2016; 29(6): 677-95. [http://dx.doi.org/10.1007/s10278-016-9884-y] [PMID: 27198133]

[96] Zhang K, Li L, Yang L, *et al.* Effect of degenerative and radial tears of the meniscus and resultant meniscectomy on the knee joint: A finite element analysis. J Orthop Translat 2019; 18: 20-1. [http://dx.doi.org/10.1016/j.jot.2018.12.004]

[97] Couteaux V, Si-Mohamed S, Nempont O, *et al.* Automatic knee meniscus tear detection and orientation classification with Mask-RCNN. Diagn Interv Imaging 2019; 100(4): 235-42. [http://dx.doi.org/10.1016/j.diii.2019.03.002] [PMID: 30910620]

[98] Byra M, Wu M, Zhang X, *et al.* Knee menisci segmentation and relaxometry of 3D ultrashort echo time cones MR imaging using attention U-Net with transfer learning. Magn Reson Med 2020; 83(3): 1109-22. [http://dx.doi.org/10.1002/mrm.27969] [PMID: 31535731]

[99] Fritz B, Marbach G, Civardi F, Fucentese SF, Pfirrmann CWA. Deep convolutional neural network-based detection of meniscus tears: comparison with radiologists and surgery as standard of reference. Skeletal Radiol 2020; 49(8): 1207-17. [http://dx.doi.org/10.1007/s00256-020-03410-2]

[100] Long Z, Zhang D, Guo H, Wang W. Automated segmentation of knee menisci from magnetic resonance images by using ATTU-Net: a pilot study on small datasets. OSA Continuum 2021; 4(12): 3096-107. [http://dx.doi.org/10.1364/OSAC.444518]

[101] Wang Y, Li Y, Huang M, Lai Q, Huang J, Chen J. Feasibility of Constructing an Automatic Meniscus Injury Detection Model Based on Dual-Mode Magnetic Resonance Imaging (MRI) Radiomics of the Knee Joint. Comput Math Methods Med 2022; 2022: 1-13. [http://dx.doi.org/10.1155/2022/2155132] [PMID: 35392588]

[102] Radiological Society of North America 2013 Scientific Assembly and Annual Meeting, Chicago IL. 2013. Available from: https://www.medscape.com/viewcollection/32980

[103] Patel R, Eltgroth M, Souza RB, *et al.* Loaded *versus* unloaded magnetic resonance imaging (MRI) of the knee: Effect on meniscus extrusion in healthy volunteers and patients with osteoarthritis. Eur J Radiol Open 2016; 3: 100-7. [http://dx.doi.org/10.1016/j.ejro.2016.05.002] [PMID: 27331081]

[104] Ozeki N, Seil R, Krych AJ, Koga H. Surgical treatment of complex meniscus tear and disease: state of the art. J ISAKOS 2021; 6(1): 35-45. [http://dx.doi.org/10.1136/jisakos-2019-000380] [PMID: 33833044]

[105] Lorigo LM, Faugeras O, Grimson WEL, Keriven R, Kikinis R. Segmentation of bone in clinical knee MRI using texture-based geodesic active contours International Conference on Medical Image Computing and Computer-Assisted Intervention. 1195-204. [http://dx.doi.org/10.1007/BFb0056309]

[106] Cohen ZA, McCarthy DM, Kwak SD, *et al.* Knee cartilage topography, thickness, and contact areas from MRI: *in-vitro* calibration and *in-vivo* measurements. Osteoarthritis Cartilage 1999; 7(1): 95-109. [http://dx.doi.org/10.1053/joca.1998.0165] [PMID: 10367018]

[107] Lynch J A, Zaim S, Zhao J, Stork A, Peterfy C G, Genant H K. Cartilage segmentation of 3D MRI scans of the osteoarthritic knee combining user knowledge and active contours. Proceedings of SPIE - The International Society for Optical Engineering 2000. [http://dx.doi.org/10.1117/12.387758]

[108] Carballido-Gamio J, Bauer JS, Keh-Yang Lee , Krause S, Majumdar S. Combined image processing techniques for characterization of MRI cartilage of the knee. Conf Proc IEEE Eng Med Biol Soc 2005; 2005: 3043-6. [http://dx.doi.org/10.1109/IEMBS.2005.1617116] [PMID: 17282885]

[109] Carballido-Gamio J, Bauer JS, Stahl R, *et al.* Inter-subject comparison of MRI knee cartilage thickness. Med Image Anal 2008; 12(2): 120-35. [http://dx.doi.org/10.1016/j.media.2007.08.002] [PMID: 17923429]

[110] Jinshan Tang , Millington S, Acton ST, Crandall J, Hurwitz S. Surface extraction and thickness measurement of the articular cartilage from MR images using directional gradient vector flow snakes. IEEE Trans Biomed Eng 2006; 53(5): 896-907. [http://dx.doi.org/10.1109/TBME.2006.872816] [PMID: 16686412]

[111] Solloway S, Hutchinson CE, Waterton JC, Taylor CJ. The use of active shape models for making thickness measurements of articular cartilage from MR images. Magn Reson Med 1997; 37(6): 943-52. [http://dx.doi.org/10.1002/mrm.1910370620] [PMID: 9178247]

[112] Gilles B, Magnenat-Thalmann N. Musculoskeletal MRI segmentation using multi-resolution simplex meshes with medial representations. Med Image Anal 2010; 14(3): 291-302. [http://dx.doi.org/10.1016/j.media.2010.01.006] [PMID: 20303319]

[113] Vincent G, Wolstenholme C, Scott I, Bowes M. Fully automatic segmentation of the knee joint using active appearance models. 2010.

[114] Williams TG, Taylor CJ, Gao Z, Waterton JC. Corresponding articular cartilage thickness measurements in the knee joint by modelling the underlying bone (commercial in confidence Biennial International Conference on Information Processing in Medical Imaging. 126-35. [http://dx.doi.org/10.1007/978-3-540-45087-0_11]

[115] Williams TG, Taylor CJ, Waterton JC, Holmes A. Population analysis of knee cartilage thickness maps using model based correspondence. IEEE Xplore 2004. [http://dx.doi.org/10.1109/ISBI.2004.1398507]

[116] Wang Z, Donoghue C, Rueckert D. Patch-based segmentation without registration: application to knee MRI International Workshop on Machine Learning in Medical Imaging. 98-105. [http://dx.doi.org/10.1007/978-3-319-02267-3_13]

[117] Liu Q, Wang Q, Zhang L, Gao Y, Shen D. Multi-atlas context forests for knee MR image segmentation International Workshop on Machine Learning in Medical Imaging. 186-93. [http://dx.doi.org/10.1007/978-3-319-24888-2_23]

[118] Schmid J, Magnenat-Thalmann N. MRI bone segmentation using deformable models and shape priors International conference on medical image computing and computer-assisted intervention. 119-26. [http://dx.doi.org/10.1007/978-3-540-85988-8_15]

[119] Schmid J, Kim J, Magnenat-Thalmann N. Robust statistical shape models for MRI bone segmentation in presence of small field of view. Med Image Anal 2011; 15(1): 155-68. [http://dx.doi.org/10.1016/j.media.2010.09.001] [PMID: 20951075]

[120] Prasoon A, Igel C, Loog M, Lauze F, Dam E, Nielsen M. Cascaded

classifier for large-scale data applied to automatic segmentation of articular cartilage. Proceedings Volume 8314, Medical Imaging 2012: Image Processing; 83144V 2012. [http://dx.doi.org/10.1117/12.910809]

[121] Huang C, Shan L, Charles HC, Wirth W, Niethammer M, Zhu H. Diseased Region Detection of Longitudinal Knee Magnetic Resonance Imaging Data. IEEE Trans Med Imaging 2015; 34(9): 1914-27. [http://dx.doi.org/10.1109/TMI.2015.2415675] [PMID: 25823031]

[122] Eckstein F, Wirth W, Nevitt MC. Recent advances in osteoarthritis imaging—the Osteoarthritis Initiative. Nat Rev Rheumatol 2012; 8(10): 622-30. [http://dx.doi.org/10.1038/nrrheum.2012.113] [PMID: 22782003]

[123] Zerfass P, Lowitz T, Museyko O, *et al.* An integrated segmentation and analysis approach for QCT of the knee to determine subchondral bone mineral density and texture. IEEE Trans Biomed Eng 2012; 59(9): 2449-58. [http://dx.doi.org/10.1109/TBME.2012.2202660] [PMID: 22692866]

[124] Youssef R, Bouhadoun H, Laredo JD, Chappard C. Semi-automatic compartment extraction to assess 3D bone mineral density and morphometric parameters of the subchondral bone in the tibial knee 2015 19th International Conference on Information Visualisation. 518-23. [http://dx.doi.org/10.1109/iV.2015.92]

[125] Lee H, Hong H, Kim J. BCD-NET: A novel method for cartilage segmentation of knee MRI *via* deep segmentation networks with bone-cartilage-complex modeling 2018 IEEE 15th International Symposium on Biomedical Imaging (ISBI 2018). [http://dx.doi.org/10.1109/ISBI.2018.8363866]

[126] Thaha R, Jogi SP, Rajan S, Mahajan V, Mehndiratta A, Singh A. Automated Segmentation of Knee Cartilage Using Modified Radial Approach for OA Patients with and without Bone Abnormality 2018 IEEE-EMBS Conference on Biomedical Engineering and Sciences (IECBES). 432-6. [http://dx.doi.org/10.1109/IECBES.2018.8626718]

[127] Uozumi Y, Nagamune K. An automatic bone segmentation method based on anatomical structure for the knee joint in MDCT image 2013 35th Annual International Conference of the IEEE Engineering in Medicine and Biology Society (EMBC). 7124-7. [http://dx.doi.org/10.1109/EMBC.2013.6611200]

[128] Desai PR, Hacihaliloglu I. Enhancement and automated segmentation of ultrasound knee cartilage for early diagnosis of knee osteoarthritis 2018 IEEE 15th International Symposium on Biomedical Imaging (ISBI 2018). 1471-4. [http://dx.doi.org/10.1109/ISBI.2018.8363850]

[129] Yamamoto Y, Tsuruta S, Kobashi S, Sakurai Y, Knauf R. An Efficient Classification Method for Knee MR Image Segmentation 2016 12th International Conference on Signal-Image Technology & Internet-Based Systems (SITIS). 36-41. [http://dx.doi.org/10.1109/SITIS.2016.15]

[130] Suresha S, Kidziński L, Halilaj E, Gold GE, Delp SL. Automated staging of knee osteoarthritis severity using deep neural networks. Osteoarthr Cartil 2018; 26(1): S441. [http://dx.doi.org/10.1016/j.joca.2018.02.845]

[131] Joseph GB, Baum T, Alizai H, *et al.* Baseline mean and heterogeneity of MR cartilage T2 are associated with morphologic degeneration of cartilage, meniscus, and bone marrow over 3years – data from the Osteoarthritis Initiative. Osteoarthr Cartil 2012; 20(7): 727-35. [http://dx.doi.org/10.1016/j.joca.2012.04.003] [PMID: 22503812]

[132] Bhagyashri LW, Patil MM. Osteoarthritis disease detection with the help of image processing technique. Int J Comput Appl 2015; 1-4.

[133] Beuf O. Characterization of trabecular bone micro-architecture in the knee in osteoarthrosis using high-resolution MRI. Clin Rheumatol 1995; 432: 16388-8.

[134] Stammberger T, Eckstein F, Englmeier KH, Reiser M. Determination of 3D cartilage thickness data from MR imaging: Computational method and reproducibility in the living. Magn Reson Med 1999; 41(3): 529-36. [http://dx.doi.org/10.1002/(SICI)1522-2594(199903)41:3<529::AID-MRM15>3.0.CO;2-Z] [PMID: 10204876]

[135] Stammberger T, Hohe J, Englmeier KH, Reiser M, Eckstein F. Elastic registration of 3D cartilage surfaces from MR image data for detecting local changes in cartilage thickness. Magn Reson Med 2000; 44(4): 592-601. [http://dx.doi.org/10.1002/1522-2594(200010)44:4<592::AID-MRM13>3.0.CO;2-J] [PMID: 11025515]

[136] Williams TG, Holmes AP, Waterton JC, *et al.* Anatomically corresponded regional analysis of cartilage in asymptomatic and osteoarthritic knees by statistical shape modelling of the bone. IEEE Trans Med Imaging 2010; 29(8): 1541-59. [http://dx.doi.org/10.1109/TMI.2010.2047653] [PMID: 20378463]

[137] Kauffmann C, Gravel P, Godbout B, *et al.* Computer-aided method for quantification of cartilage thickness and volume changes using mri: validation study using a synthetic model. IEEE Trans Biomed Eng 2003; 50(8): 978-88. [http://dx.doi.org/10.1109/TBME.2003.814539] [PMID: 12892325]

[138] Swanson MS, Prescott JW, Best TM, *et al.* Semi-automated segmentation to assess the lateral meniscus in normal and osteoarthritic knees. Osteoarthritis Cartilage 2010; 18(3): 344-53. [http://dx.doi.org/10.1016/j.joca.2009.10.004] [PMID: 19857510]

[139] Folkesson J, Dam E, Olsen OF, Pettersen P, Christiansen C. Automatic segmentation of the articular cartilage in knee MRI using a hierarchical multi-class classification scheme International Conference on Medical Image Computing and Computer-Assisted Intervention. 327-34. [http://dx.doi.org/10.1007/11566465_41]

[140] Folkesson J, Olsen OF, Pettersen P, Dam E, Christiansen C. Combining binary classifiers for automatic cartilage segmentation in knee MRI International Workshop on Computer Vision for Biomedical Image Applications. 230-9. [http://dx.doi.org/10.1007/11569541_24]

[141] Gornale SS, Patravali PU, Marathe KS, Hiremath PS. "Determination of Osteoarthritis Using Histogram of Oriented Gradients and Multiclass SVM," Int. J. Image. Graph Signal Process 2017; 9(12): 41-9. [http://dx.doi.org/10.5815/ijigsp.2017.12.05]

[142] Ang I, Fox M, Polk JD, Kersh ME. A structure-based algorithm for automated separation of subchondral bone in micro-computed tomography data. Preprint 2018. [http://dx.doi.org/10.31224/osf.io/w86ke]

[143] Li YZ, Wang Y, Fang KB, *et al.* Automated meniscus segmentation and tear detection of knee MRI with a 3D mask-RCNN. Eur J Med Res 2022; 27(1): 247. [http://dx.doi.org/10.1186/s40001-022-00883-w] [PMID: 36372871]

[144] Fripp J, Bourgeat P, Mewes AJ, Warfield SK, Crozier S, Ourselin S. 3D statistical shape models to embed spatial relationship information International Workshop on Computer Vision for Biomedical Image Applications. 51-60. [http://dx.doi.org/10.1007/11569541_7]

[145] Litjens G, Toth R, van de Ven W, *et al.* Evaluation of prostate segmentation algorithms for MRI: The PROMISE12 challenge. Med Image Anal 2014; 18(2): 359-73. [http://dx.doi.org/10.1016/j.media.2013.12.002] [PMID: 24418598]

[146] Janvier T, Toumi H, Jennane R, Lespessailles E. Subchondral tibial bone texture predicts the incidence of radiographic knee osteoarthritis: Data from the osteoarthritis initiative. Osteoarthr Cartil 2017; 25(12): 2047-54.

[147] Maly MR, Acker SM, Totterman S, *et al.* Knee adduction moment relates to medial femoral and tibial cartilage morphology in clinical knee osteoarthritis. J Biomech 2015; 48(12): 3495-501. [http://dx.doi.org/10.1016/j.jbiomech.2015.04.039] [PMID: 26141161]

[148] Hossain MB, Lai KW, Pingguan-Murphy B, Hum YC, Mohd Salim MI, Liew YM. Contrast enhancement of ultrasound imaging of the knee joint cartilage for early detection of knee osteoarthritis. Biomed Signal Process Control 2014; 13(1): 157-67. [http://dx.doi.org/10.1016/j.bspc.2014.04.008]

©2024 The Author(s): Published by Bentham Science Publisher.

This is an open access article distributed under the terms of the Creative Commons Attribution 4.0 International Public License (CC-BY 4.0), a copy of which is available at: https://creativecommons.org/licenses/by/4.0/legalcode. This license permits unrestricted use, distribution, and reproduction in any medium, provided the original author and source are credited.